

## RESPONSE TO REVIEW #1 OF GMD MANUSCRIPT:

### “Introducing the Probabilistic Earth-System Model: Examining The Impact of Stochasticity in EC-Earth v3.2”

We thank the reviewer (hereby referred to as Reviewer #1) for their comments, which have helped us improve the clarity and quality of our manuscript.

#### MAJOR POINTS

- 1) **Reviewer #1:** *The order of the figures needs to be revised. (E.g. line 17, page 7, Figure 3 is mentioned before Figure 2).*

**Our response:** Yes, this was a clear oversight on our part. The revised manuscript now has figures numbered in the order they appear.

- 2) **Reviewer #1:** *“Some choices in the implementation of the stochastic perturbation needs to be motivated. For example what is the motivation behind the 3 temporal and spatial scales associated to STTP and ISTTP (Line 8, page 4). Also why the amplitude of the multiplicative perturbation factor is tapered in the boundary layer (given that the PBL scheme is a source of the kind of model errors that the stochastic perturbations are trying to represent?). Another choice that is not motivated is the use of parameter perturbation instead of stochastic tendency perturbation in the LAND experiment (Section 2.3).”*

**Our response:** We initially omitted some of these details for the sake of brevity, as most of the answers are covered in the cited papers. In response to this comment, we have now addressed these questions in the revised manuscript. The answers are as follows.

The three temporal and spatial scales associated to the SPPT/ISPPT perturbations come from the assumption that model error can come both from processes that happen at very fast timescales (and, therefore, small spatial scales), and also, independently, for processes happening on very slow timescales (and, therefore, large spatial scales). The three patterns are a compromise aimed at capturing a plausible range of relevant atmospheric processes.

The tapering in the boundary layer was implemented due to model stability issues. Numerical instabilities begin to accumulate when perturbations are added in the lowest model levels due to the delicate balance between model dynamics and vertical transport in this region.

Finally, for the stochastic land scheme, in fact tendency perturbations had been tested initially, but were found to have little to no impact on soil moisture in the model.

Parameter perturbations were therefore done instead, as these produce changes in soil moisture that more plausibly capture the model uncertainties.

- 3) Reviewer #1:** *“What is the motivation behind using the same perturbation for convection and large scale condensation in the ISPPT approach? The tendencies produced by these parametrizations are sometimes anti-correlated since when convection fails to remove instability from an atmospheric column large scale condensation tries to do that.”*

**Our response:** In the IFS, which forms the atmospheric component of EC-Earth, moist processes are split up into convection and large-scale condensation. The convection scheme transports moisture aloft, where it is detrained. This forms an input to the large-scale condensation scheme, which determines whether supersaturation has been reached and therefore how much cloud should be present. If needed, it then removes water vapour from the atmosphere with a corresponding increase in liquid water content. The intimate relationship between convection and large-scale condensation, whereby the outputs from one form the inputs to the other, motivated us to perturb these schemes together. Tests in an NWP setting indicate that grouping moist processes in this way gave skilful weather forecasts (Christensen et al, 2017, QJRMets).

- 4) Reviewer #1:** *“It would be good to provide more discussion about the pathways in which the stochastic perturbations can change the mean. I agree in that the impact of SPPT and ISPPT suggests that the convective scheme is activated more frequently, however the discussion on how the stochastic perturbations can lead to this is not clear (e.g. line 14, page 10). In the discussion section it is stated that some perturbations can trigger convection in areas in which the unperturbed state has conditions close to those required to activate the convective scheme. However the opposite is also possible, some columns in which the unperturbed state is sufficient for the initiation of deep moist convection can be perturbed leading to a state in which these conditions are not met any more.”*

**Our response:** We would like to clarify that we do not assert that SPPT/ISPPT necessarily would be expected to trigger convection more or less frequently. Rather, our main assertion is that the inherent asymmetry in condensation triggers means that even a totally symmetric perturbation could lead to an increase in the mean cloud water content. This is because, while a perturbation away from e.g. deep moist convection would not be expected to change the cloud water content in the column (for that timestep), a perturbation towards it may trigger water to condense, which increased cloud water content. In other words, the impact of symmetric perturbations would be expected, if anything, to increase cloud water.

This increase in cloud water is suggested as a leading order mechanism (or pathway) towards larger scale changes with SPPT/ISPPT. This hypothesis is explained in the original manuscript on page 14, lines 9-16 (see the whole paragraph for a full discussion).

The comment the reviewer refers to (line 14, page 10) is specifically about precipitation *extremes*, which had been observed to increase with SPPT in previous studies. This was suggested as a potentially important pathway towards the observed changes in soil moisture.

The revised manuscript now contains some clarifying remarks to this effect in both sections.

- 5) **Reviewer #1:** *“As part of a first evaluation of the impact of SPPT, ISPPT and LAND upon the EC-Earth model it would be good to present some scores related to atmospheric circulation. Like for example MSE and biases for wind at different atmospheric levels and also for temperature at these same levels. The goal of the paper is focused on surface fluxes, but atmospheric circulation is also examined by studying for example the impact upon the Hadley cell. Although the impact upon the Hadley cell is relevant (particularly because SPPT and ISPPT seems to produce a large impact upon tropical convection), it would be good to provide these other scores for comparison with other systems.”*

**Our response:** We thank the reviewer for the suggestion, which we agree would be a helpful way to allow for easy comparison with other studies. We have extended Table 2 to add the MSE of temperature and zonal wind fields at various levels. This also helps illuminate the reviewer’s next question, and our answer to it.

- 6) **Reviewer #1:** *“It is not clear for me what is the motivation to study the QBO in the context of this paper. I understand that the impact upon different aspects of the atmospheric dynamics should be investigated but the inclusion of this particular aspect in a first evaluation has to be better motivated.”*

**Our response:** The reviewer makes a good point: this was not adequately motivated. Our primary motivation here comes from the paper Leutbecher et al. (2017), *Stochastic representations of model uncertainties at ECMWF: State of the art and future vision*, where the impact of SPPT on short to medium range forecasts is considered. On page 11 of this paper, it is documented that the biggest degradation of SPPT on the version of the IFS considered is on the upper level winds, where the QBO dominates. The MSE computations we added in Table 2 (c.f. our response to the previous comment) show similar behaviour. This is raised in *ibid* as being a point of concern due to the growing body of literature suggesting that the QBO is an important driver of European climate at seasonal timescales. We therefore wished to identify if a similar degradation occurs in the EC-Earth model for the schemes considered.

We have now added this motivation to the introduction of section 7.

## MINOR POINTS

- 1) **Reviewer #1:** *“Line 10, page 5. What does exactly mean that parameters are correlated? Estimated parameters based on observation studies show that the value of these parameters in different soil types and conditions are correlated or that the joint sensitivity of these two parameters shows a certain degree of compensation between the impact of these two parameters (i.e. the effect of the increase in one of the parameters can be compensated by changes in the other parameter).”*

**Our response:** We meant the former. Estimations of parameters based on observation studies indicate that the two parameters show correlation across soil types. This correlation is neither zero nor one, indicating that the parameters are related whilst showing some independence. We therefore chose not to perturb the two parameters with the same pattern, nor with two entirely independent patterns. Rather, we introduce some dependence between the perturbations through definition of a third pattern, as described in the text.

The rationale for this is that the observed correlation suggests that some parts of parameter space may be unphysical (for instance extremely high values of gamma and low values of alpha). An independent perturbation would be likely to access these regions of parameter space (for instance simultaneous values of  $1+r=1.8$  for gamma and  $1+r=0.1$  for alpha). By tethering both parameters to a third base pattern, this possibility is reduced and the parameters are perturbed in a more similar way, whilst retaining some independence in the perturbation.

We have slightly rephrased the description in this section to make it clear that the correlation is based on observational studies.

- 2) **Reviewer #1:** *“Why performing 5 periods of 20 years each instead of a longer simulation. Using 5 different periods as ensemble members can artificially increase the ensemble spread and reduce the significance of the results. Also spin-up issues may be more important when several shorter periods are considered, particularly in the soil variables.”*

**Our response:** When constructing the experimental protocol, the authors recognized that there were several aspects it would be good to test, but that there were insufficient computer units to run all the configurations desired. We decided that the most important goal was to produce runs where the significance of any impacts could best be detected: for this reason, it was decided to produce an ensemble of simulations for each scheme as opposed to a single long run. The authors believe that comparison of distinct ensemble members allows for the most transparent and accurate assessment of the uncertainty in the computed metrics. While such an assessment from a single longer run would be possible by using techniques such as subsetting the data and/or bootstrap resampling, these techniques are essentially just trying to artificially create distinct ensemble members within the longer timeseries anyway. Therefore, simply producing an actual ensemble from definitely distinct initial conditions gives the cleanest methodology, in our opinion. We are not aware of any

reason why this may increase the spread in a way which is excessive compared to that diagnosed with other experimental protocols.

The initialisation of each ensemble member to a slightly different time period also allows us to cleanly assess any dependence of the rapid response on the initial ocean and land state. Spin up issues may have been expected to be problematic for the land state, but in practice we found that the main changes were the same across all the time periods, implying that the impact of the schemes are quite rapid and do not require a longer period to assess accurately.

We have included some more discussion on why our experimental protocol was chosen, based on the above discussion, in the revised version of the paper and hope that this will satisfy the reviewer.

**3) Reviewer #1:** *“Line 29, page 4. Remove parenthesis and “for details”.”*

**Our response:** We made the suggested change.

**4) Reviewer #1:** *“Line 29, page 6. Missing space before Spatial. Also indicate instead of indiate.”*

**Our response:** We made the correction.

**5) Reviewer #1:** *“Since convective precipitation is part of the products generated by the convective scheme and is linked to the other tendencies, is precipitation rate perturbed in the same way as the other tendencies produced by the parametrization? Same question but for the large scale condensation scheme.”*

**Our response:** Thank you for your insightful question. You are right, for complete consistency the fluxes in precipitation and evaporation should be perturbed using the same pattern as for SPPT. However, this is not currently implemented in SPPT. This could be part of the reason why the scheme does not conserve water, which is why the ‘humidity fix’ has been implemented to correct this. Having said that, testing is underway to develop a more consistent approach whereby precipitation and evaporation are perturbed, to bypass the need for the ‘humidity fix’.

**6) Reviewer #1:** *“Line 6 page 14. More frequent convective scheme activation can also explain why the PBL is drier.”*

**Our response:** We thank the reviewer for the insightful comment: we have added a comment on this in this section of the revised manuscript.

- 7) **Reviewer #1:** *“Figure 4 a, shows the biases in the precipitation for the control run. This bias pattern is strong and shows a clear maximum in the tropics. The authors indicate that the control configuration has been extensively tuned, however has the tuning been performed with this same model resolution?”*

**Our response:** The model was indeed tuned at the T255 spectral resolution which we used in this study. The tuning procedure for EC-Earth is carried out in order to obtain a realistic energy budget, with a particular focus on the net surface energy flux. In particular, precipitation biases are not directly tuned. Therefore, while the deterministic model has little bias in the energy fluxes at the surface, it does still have relatively notable biases in key variables like precipitation.

- 8) **Reviewer #1:** *“Line 16, page 15. Changes in the Hadley cell are caused by changes in evaporation? Or these two changes are driven by changes in tropical convection?”*

**Our response:** The reviewer makes a good point; the manuscript as it stood focused on changes to evaporation (latent heat flux) because of the focus on energy budget changes. However, it is of course possible that the first order impact is on tropical convection, and evaporation changes are a response to this. We have included some discussion of this in section 8.1 (Discussion) and 8.2 (Conclusions).

- 9) **Reviewer #1:** *“Figure 6: The changes in T2m over the sea ice in the ISPPT and LAND are very strong. It is surprising to see these changes in both experiments since none of these experiments seems to directly affect the sea-ice parametrization in any way (SPPT for example do not show a strong change in bias in this region). I suggest to check the sea-ice distribution and temperature in these experiments.”*

**Our response:** Being AMIP style experiments, the sea-ice distribution is a fixed field along with the sea-surface temperatures. Therefore, for both ISPPT and LAND, the cooling seen in the sea-ice regions are necessarily induced via atmospheric circulation changes, which can cause surface temperature (which is dynamic) to change. Discussion of potential mechanisms behind atmospheric circulation changes are included in the manuscript, and have been extended upon based on other comments by both reviewers. We therefore do not expand upon this further.

**10) Reviewer #1:** *“Figure 11. I suggest to use the same names as in the rest of the manuscript.”*

**Our response:** We made the suggested change.

**11) Reviewer #1:** *“Figure 8. Please correct the caption since the colors do not correspond to the ones on the legend (I assumed that the legend is correct).”*

**Our response:** We thank the reviewer for pointing out this silly mistake on our part. The caption has been edited to match the legend in the figure.

**12) Reviewer #1:** *“Line 10, page 8. This sentence is not clear, I can not see “each model simulation” but something that seems to be the mean of all simulations”*

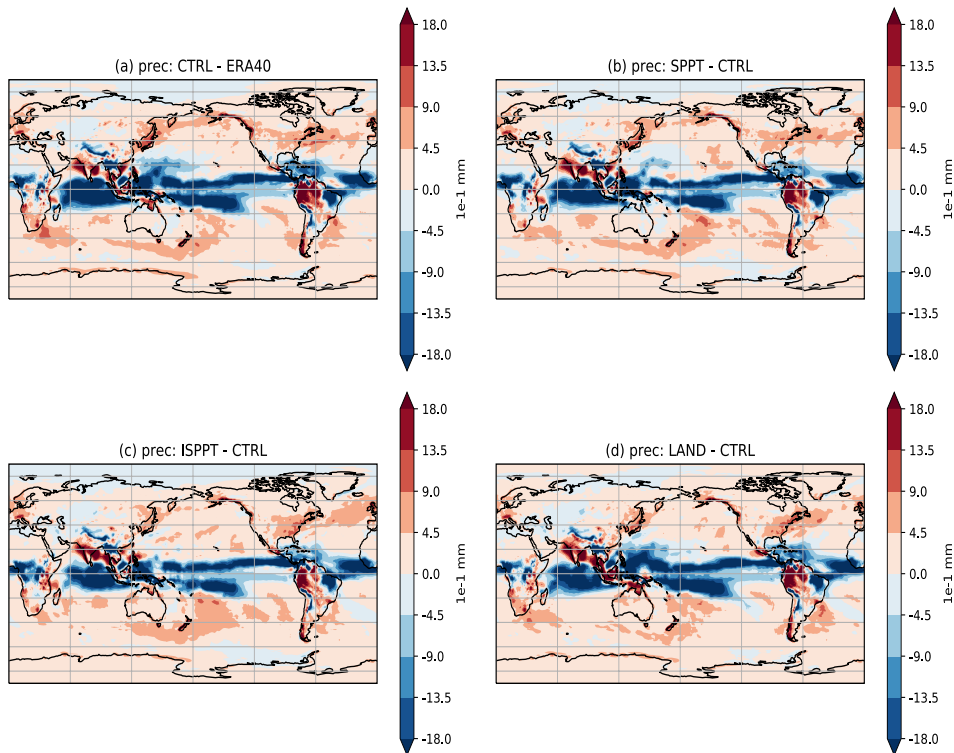
**Our response:** Our phrasing was somewhat unclear. We meant ‘the mean across all the individual differences’. We have rephrased this as follows: ‘Figure 8(a) shows the mean difference between the five SPPT-simulations and the corresponding CTRL-simulations (i.e. the average across the 5 differences), ...’

We hope this rephrasing makes the meaning clearer.

**13) Reviewer #1:** *“It would be better to use the same color scale for all panels in figures 3, 4, 5, 6 and 7. In most cases the range is similar. Another possibility is to show in all cases the bias with respect to ERA (again since the magnitudes are similar this should clearly show the improvement produced by the stochastic schemes and would be more easy to analyze). Also in this figures indicate what “M=” stands for. I assumed that this is the mean bias over the global domain.”*

**Our response:** We have added the explanation for “M=” in the captions now, a clear oversight: the reviewer was indeed correct in their assumption of its meaning.

We would like to respectfully disagree with the reviewer on the suggestion to change the spatial maps to show the bias with respect to ERA in each panel, as we believe this would make it harder, not easier, to analyse. As an example, consider the precipitation changes in figure 4. Note that the CTRL bias is nearly 3 times as large in magnitude as the impact of the stochastic schemes (with the former having a peak of ~1.8mm and the latter a peak of ~0.6mm). As a result, showing ERA biases side by side is not very illuminating, as the following figure demonstrates:



Showing the bias relative to CTRL immediately illuminates how the scheme is changing the mean state for all the variables. Colourscales are tailored specifically to each individual variable, and chosen so that the scale encapsulates 2 standard deviations around the mean bias. For a more easily comparable quantitative metric, we have used the mean bias (M=...) and the MSE table. We therefore suggest to leave the figures as they are.

**14) Reviewer #1:** *“Since the main goal is to perform analysis towards the development of a coupled stochastic modeling system, why a SPPT+LAND or ISPPT+LAND experiments where not performed?”*

**Our response:** In fact, such experiments were carried out. These were not ultimately included in the analysis proper, because the impact of SPPT/ISPPT is typically much larger in magnitude than the impact of LAND, which makes it difficult to assess the individual impact of either in a joint experiment. This piece of information should clearly have been included in the paper, and we thank the reviewer for making this point. We have now added a paragraph on this in the Experimental Setup section (section 3.1).

## RESPONSE TO REVIEW #2 OF GMD MANUSCRIPT:

### “Introducing the Probabilistic Earth-System Model: Examining The Impact of Stochasticity in EC-Earth v3.2”

We thank the reviewer (hereby referred to as Reviewer #2) for their comments, which have helped us improve the clarity and quality of our manuscript.

- 1) **Reviewer #2:** *“Title: the title mentions the “Probabilistic Earth-System Model” while indeed all work has been done entirely with the atmosphere component of EC-Earth only. In my eyes the title this suggests more than what the manuscript delivers and to avoid any too far reaching expectation I’d therefore suggest to modify the title to something more adequate.”*

**Our response:** The reviewer makes a fair point. We have now edited the title to “Progress Towards a Probabilistic Earth System Model: Examining The Impact of Stochasticity in EC-Earth v3.2”, reflecting the paper as a natural step from the vision outlined in Palmer (2012), “Towards the probabilistic Earth system simulator”. This should be more in line with the actual content of the paper.

- 2) **Reviewer #2:** *“Section 2.1, 1st paragraph: there is no need to go into details about EC-Earth’s ocean component or coupler because they are irrelevant in this work.”*

**Our response:** We have removed these details.

- 3) **Reviewer #2:** *“Section 2.2, eq 1: what is “the i’th physics parameterization scheme”? You mention the schemes explicitly towards the end of Sec 3.1, why don’t you list them here already?”*

**Our response:** We have now explicitly identified the different physics schemes in section 2.2.

- 4) **Reviewer #2:** *“Section 2.2, eq 1: are the tendencies for all variables perturbed by the same  $r$ ? Or are there different perturbations for the different variables?”*

**Our response:** All variables are perturbed in the same way: the tendency vector  $P$  has, as its entries, the tendencies for temperature, humidity, and wind fields. It is this vector which is perturbed, implying that all variables are perturbed similarly. We have slightly rephrased the explanation of what  $P$  is to emphasize that it contains all these tendencies to clarify this point.

5) **Reviewer #2:** *“Section 2.2, eq 1: are the perturbations constant in time, or do they vary from one timestep to the next?”*

**Our response:** The perturbations evolve over time as AR(1) processes. We have rephrased the presentation slightly in response to this point, emphasizing both that the perturbation happens at each timestep, and that the perturbation  $r$  evolves in time.

6) **Reviewer #2:** *“Section 2.2, end of 1st paragraph: you say “perturbation is limited between 0 and 2” but shouldn’t that be between -1 and 1? Even with  $r=-1$  we still get that  $P_{\hat{}}$  has the same sign as  $P$ , or?”*

**Our response:** This was incorrectly phrased on our side: the reviewer is entirely correct that  $r$  itself is clipped between -1 and 1: this implies that  $1+r$  is clipped between 0 and 2, which is why this range was referenced in the submitted manuscript. We have revised the script accordingly.

7) **Reviewer #2:** *“Section 3.1, p.6 l.13: why do you use ERA-40 or ERA interim for the evaluation? These re-analysis datasets belong to the same model “family” as EC-Earth and may therefore share common biases, in particular where the re-analysis are largely a model product not constrained by observations. I would prefer the evaluation to be done against a different re-analysis dataset, but that may be too much to ask for at this stage. In any case, it would be good if the similarity between EC-Earth and the model used for the re-analysis would be clearly stated.”*

**Our response:** The reviewer makes a good point. Experience suggests this is unlikely to be an issue for surface variables such as surface temperature which are strongly constrained by existing observations and therefore do not differ much across reanalysis datasets. However, certain less strongly constrained variables, such as total cloud cover (considered in the paper) may be more affected by this, so we agree it is important to point out.

We have now added a disclaimer addressing this point in section 3.1 covering this point, and we hope the reviewer will find this sufficient.

**8) Reviewer #2:** *“Section 3.4: how good is it to compare only the last 10 (5) years from the last ensemble member against observations? Is that short time period really sufficient to confirm or reject the fitness of EC-Earth? I don’t understand why you don’t average 10-20 year from all ensemble members (start dates) and compare against the corresponding time period of the re-analysis (see also comment above about choice of re-analysis data).”*

**Our response:** The reviewer makes a very reasonable point. As implied in the manuscript, we restricted our assessment to this time period because the default CTRL version of the model was tuned for this particular time period. The reason for restricting attention to this shorter time period is a decision made by the EC-Earth Consortium as a whole, but I believe it is to avoid the possibility of ‘fitting’ the model’s climate sensitivity. If one tries to match the energy budget over a long time period, one is effectively trying to fit the specific temperature growth, i.e. the climate sensitivity over the historical period. Fitting therefore to a very recent time period, where there is good satellite data for robust observational estimates, is therefore a pragmatic choice for model tuning.

One key conclusion drawn from this paper is that the model will in general need to be retuned after the addition of stochastic schemes, and that for this reason, comparisons of a scheme’s performance against the CTRL model must always be considered with respect to the model’s tuning procedure. In particular, because EC-Earth is tuned according to the historical time periods energy budget, the performance of a stochastic scheme on the energy budget over the same period will almost always look like a degradation. This is why, when comparing to observations, we only explicitly considered the short time period in question.

It is true that we could nevertheless have considered the evolution of the energy budget over the full simulation period 1960-2000. However, this essentially amounts (as explained above) to assessing the impact of the schemes on the model’s climate sensitivity. This was not a topic we wanted to expand upon in this manuscript, because it is the topic of an independent manuscript currently under review (Strommen et al 2019, now cited in the revised manuscript). We have added a caveat to this effect in Section 3.4.

**9) Reviewer #2:** *“Section 4,5,6: when you talk about cloud water do you mean the gridpoint value of the in-cloud value? I would suspect it’s the gridpoint value, and if that’s the case then the reduction in cloud cover would imply an even larger increase in the in-cloud water content with all the consequences for optical thickness and cloud microphysics. Good if you could clarify on this point.”*

**Our response:** Cloud liquid water refers to the vertical integral of liquid water contained within clouds in a single gridpoint column: we have added this descriptor to the revised manuscript in response to the reviewers point.

The point about reduced cloud cover further ‘exacerbating’ the increased cloud water content is a good one. We have included a line to this effect in the revised manuscript, section 4.1.

**10) Reviewer #2:** *“Section 4.2,5.2,6.2 and Fig 8: I don’t see a point in making a timeseries of the energy budget, the interesting aspect for a climate model is how well it simulates the average flux and its variability compared to observations (re-analysis). For that reason it would make more sense to average the biases in the fluxes and present them as a table or barplot similar to how you did in Figs 1 and2.”*

**Our response:** While we agree with the reviewer that the most important aspect is the model’s ability to capture the average flux and variability compared to observations, the timeseries plot does capture some relevant further information. Because the differences are effectively constant in time, this implies that the impact is not independent of the initial ocean state. Furthermore, one can infer that the model adjustment is extremely rapid, with the stochastic schemes not causing any systematic drift; because of the potentially slow response of the land-scheme, such drift cannot be ruled out a priori even in the absence of ocean coupling. Therefore, we feel there is value in keeping this as a timeseries plot.

We do however accept that the above reasoning was not adequately included in the submitted manuscript. We have added a brief comment to this effect in sections 4.2, 5.2 and 6.2 (Energy Budget impact sections for the three schemes).

**11) Reviewer #2:** *“Section 7: what is the motivation for selecting the Hadley circulation and the QBO as test cases for the stochasticity? Why not NAO or PNA as other prominent modes of atmospheric variability?”*

**Our response:** In response to a comment by Reviewer #1, we have added motivation for these choices in the revised manuscript: see the introduction to Section 7.

**12) Reviewer #2:** *“Section 7.1 Fig 9: It is not easy to easy to distinguish the different colors of the dots (I am slightly color blind) and you should consider presenting the data in a different way, e.g. by using different symbols for the different members/time periods.”*

**Our response:** We have edited Figure 9 to make the points be larger and use different symbols; we also added a legend to aid interpretation. The colourscale has been chosen due specifically to its readability for colour blind people: if the reviewer still finds the plot tricky to parse, then we would be very happy to edit it further !

**13) Reviewer #2:** *“Section 7.2: what is the reason for evaluating QBO only for the last ensemble member? Why not using the results from all start dates?”*

**Our response:** We were not clear enough in the presentation of this section. To be clearer, the estimate of the QBO period for the simulations are done using all 5 ensemble members: the period shown is the average across these 5 estimates. For Figure 11, showing a pressure-time contour plot, we only show this for the last ensemble member because the degraded QBO looks extremely similar across all 5 members. Therefore, we opted to simply show the last member as an example, against the more recent ERA-Interim reanalysis data.

We have added some clarifying remarks to this effect in Section 7.2, in response to this point. In addition, we have included errorbars in the QBO period plot, to show the spread across the 5 estimates. This illuminates the results further and immediately suggests that the full ensemble is used for the computation.

**14) Reviewer #2:** *“Section 8, 1st sentence: you cannot blame the absence of a more process-oriented analysis on the lack of available data because you have designed the experiment and its output.”*

**Our response:** Yes, you are of course right. The point is rather that we made an explicit choice to construct experiments that would illuminate changes in the long-term climate, and therefore did not construct an experimental protocol that was suitable for robust assessment of the rapid response of the model. We have rephrased the introduction to Section 8 to clarify this.

We further point out there, that experiments aimed at illuminating the rapid response of the model to SPPT were carried out in Strommen et al (2019). These in fact appear to confirm the hypothesis made in the present paper, as they show that the very rapid response is to cloud liquid water and evaporation.

**15) Reviewer #2:** *“Section 8.1, p.14 l.7: it’s not clear to me how an increased in-cloud liquid water content could steepen the near-surface humidity gradient. Could you explain better what you mean?”*

**Our response:** This was poorly phrased on our part. We have rephrased this part of section 8.1 in response to questions from Reviewer #1, and it is hopefully more illuminating now. For your convenience, this paragraph now reads:

“With both SPPT and ISPPT, the dominant impact on the energy budget is increased evaporation. In the IFS, the amount of evaporation at a gridpoint depends primarily on the surface wind-speeds and the extent to which the specific humidity at the surface gridpoint differs from the saturation humidity (a function of surface temperature). While wind-speeds do increase by about 1.4% on average with ISPPT, the mean wind-speeds are unchanged with SPPT, with a tiny increase of only 0.06%. Given that the increase in evaporation of both SPPT and ISPPT are of the same order of magnitude, this suggests changes in humidity are a key factor. Because SST's are held fixed, such changes will be, to first order, driven by changes in the water content of the atmosphere as opposed to temperature changes at the surface. One possibility is that the increase in cloud liquid water is depleting the near-surface humidity, causing more favourable conditions for evaporation. The fact that both

cloud liquid water and surface wind-speeds increase more with ISPPT could then explain why this impact is amplified in those experiments. Another possibility is that the first order impact is on convection in the tropics, which may be activated more frequently with SPPT/ISPPT. This could lead to a drying of the boundary layer, promoting more evaporation in response.”

**16) Reviewer #2:** *“Section 8.2, p.15 l.13: what do you mean with runoff being a key driver of atmosphere interaction? Isn’t runoff simply the difference between P-E and the amount of water absorbed by soil? It’s a residual, not a driver, or?”*

**Our response:** It would indeed be more correct to say that soil moisture is the key conduit between the land and the atmosphere, through its impact on evaporative cooling and latent heat transfer. The point we are trying to make in the manuscript is that the primary impact of the LAND scheme is to affect runoff, and the changes in runoff lead to changes in soil moisture and, hence, the atmosphere as a whole.

Note that because the scheme is perturbing parameters in the soil equations themselves, it is possible for the scheme to change runoff *directly*. Note also that while *surface* runoff is effectively a residual, *subsurface* runoff in the land surface model is generated through a free drainage condition, which is dependent on soil hydrology parameters.

**17) Reviewer #2:** *“Section 8.2, p.15 l.22: why do you call runoff a tuning parameter in the LAND case? Runoff is an important diagnostics of the model that can be used to tune the model, but runoff itself isn’t a tuning parameter.”*

**Our response:** There seems to be a misunderstanding here. Our statement is “Tuning parameters for EC-Earth **include constants that regulate** [...] **runoff** in the LAND scheme case” (bolded for emphasis). In other words, we absolutely agree that runoff itself isn’t a parameter that can be tuned, but other actual tuning parameters have a strong impact on the behaviour of runoff in the model, and these parameters *are* tuned.

We have therefore left this statement as is in the revised manuscript.

**18) Reviewer #2:** *“Code availability: EC-Earth is licensed and not openly available, it’s not sufficient for any presumptive user to request access. I would suggest you check the guidelines of GMD that regulate code availability and re-phrase this section.”*

**Our response:** Yes, this should have been made clearer. We did state that access was available upon requesting permission from the consortium, but should have been clearer that this is due to explicit licensing issues attached to the IFS component. We have now rephrased this.

**19) Reviewer #2:** *“p.2 l.12: “However” seems to be inappropriate in this sentence.”*

**Our response:** We agree, and have rephrased this to “Most modern climate models also ...”.

**20) Reviewer #2:** *“p.15 l.15: shouldn’t it rather be “...none of the schemes \_is\_ able...”?”*

**Our response:** This particular grammatical construction is one of those funny English loose ones, where I believe one can get away with using either ‘is’ or ‘are’. However, when the meaning is ‘none of them’, one typically uses the plural ‘are’.

# List of changes

The following list outlines all the main changes in the revised manuscript. These are highlighted in red in the marked version of the manuscript.

1. The title was changed.
2. Details of ocean component were removed due to lack of relevance.
3. Details were added to the description of the SPPT scheme. Details of the ‘humidity fix’ were added and discussed.
4. Extended motivation for the choice of our experimental protocol.
5. Added motivation for our configuration of the ISPPT scheme.
6. Disclaimer added concerning the use of ERA reanalysis data (which use the IFS) for comparison with an IFS based climate model.
7. Included mention of the combined experiments (SPPT+LAND, ISPPT+LAND) carried out.
8. Added further discussion on why we restricted explicit numerical energy budget comparisons to the 1990-2000 period.
9. Clarified the definition of ‘cloud water’, and further emphasis on the relative impact of increased cloud water and reduced cloud cover.
10. Added points to emphasize how the constant differences in energy budget quantities implies no dependency on the initial ocean state as well as lack of any spin-up in the land scheme (soil moisture etc.)
11. Clarification on the mechanism of runoff changes with ISPPT.
12. Added motivation for choosing to focus on the Hadley Cell and the QBO for atmospheric circulation changes.
13. Changes to discussion of QBO. Clarification of the use of all ensemble members and discussion of uncertainty of estimated QBO periods.
14. Fairly extensive changes to the discussion section with further clarifications on potential pathways of circulation changes due to the stochastic schemes.

15. Edits to the EC-Earth code availability.
16. Changes to figures; order has changed to be numbered in the order referred to in text; corrections to some errors in legends; added explanation of the "M=" mean bias changes; improved readability of Hadley cell plots; added errorbars to the QBO period plot.

# Progress Towards a Probabilistic Earth System Model: Examining The Impact of Stochasticity in EC-Earth v3.2

Kristian Strommen<sup>1</sup>, Hannah M. Christensen<sup>1</sup>, Dave MacLeod<sup>1</sup>, Stephan Juricke<sup>2,3</sup>, and Tim N. Palmer<sup>1</sup>

<sup>1</sup>Department of Atmospheric, Oceanic and Planetary Physics, Oxford University, Oxford, UK.

<sup>2</sup>Alfred Wegener Institute, Helmholtz Centre for Polar and Marine Research, Bremerhaven, Germany.

<sup>3</sup>Jacobs University Bremen, Bremen, Germany.

**Correspondence:** Kristian Strommen (kristian.strommen@physics.ox.ac.uk)

**Abstract.** We introduce and study the impact of three stochastic schemes in the EC-Earth climate model, two atmospheric schemes and one stochastic land scheme. These form the basis for a probabilistic earth-system model in atmosphere-only mode. Stochastic parametrisations have become standard in several operational weather-forecasting models, in particular due to their beneficial impact on model spread. In recent years, stochastic schemes in the atmospheric component of a model have been shown to improve aspects important for the models long-term climate, such as ENSO, North Atlantic weather regimes and the Indian monsoon. Stochasticity in the land-component has been shown to improve variability of soil processes and improve the representation of heatwaves over Europe. However, the raw impact of such schemes on the model mean is less well studied, It is shown that the inclusion of all three schemes notably change the model mean state. While many of the impacts are beneficial, some are too large in amplitude, leading to significant changes in the model's energy budget and atmospheric circulation. This implies that in order to keep the benefits of stochastic physics without shifting the mean state too far from observations, a full re-tuning of the model will typically be required.

## 1 Introduction

One of the key guiding principles of the scientific method is the need to assess and quantify uncertainty. The truncation of the true climate system to a finite grid necessarily introduces a large source of uncertainty from unresolved sub-grid scale processes. While parametrisations are usually developed to account for these unresolved processes (Bauer et al., 2015), the parametrisation process relies on introducing a number of simplifications and assumptions that are not always valid, effectively introducing an additional layer of uncertainty in any model prediction (Palmer et al., 2005). Some of these assumptions are resolution-dependent: for example, convection parametrisations typically assume that the size of a grid-box is large enough for the grid box to contain a large sample of clouds, such that the average influence of the clouds is well constrained by the resolved flow (Arakawa and Schubert, 1974; Lord et al., 1982). As model resolution continues to increase, such assumptions can become increasingly tentative, even while the resolution is still far from being explicitly cloud resolving. The need to represent the uncertainty of the sub-grid contribution to the flow therefore becomes increasingly important.

In medium-range and seasonal forecasts using numerical weather prediction models, the use of stochastic schemes has become widespread as a means to sample this uncertainty. Studies have shown that when properly calibrated, such schemes

have a beneficial impact on both the spread and mean state of these forecasts (Weisheimer et al., 2011; Berner et al., 2017; Leutbecher et al., 2017). In recent years, there has been increasing interest in understanding the impact of these schemes also on the long-term climate of a model. In Palmer (2012), it was argued that introducing stochasticity into climate models may be a key step towards eliminating persistent model biases and reducing uncertainty in climate projections. Since then, the insertion of a stochastic component into a climate model has been demonstrated to improve several key processes, including El Niño-Southern Oscillation (Christensen et al., 2017a; Yang et al., 2018; Berner et al., 2018), the Madden Julian Oscillation (Wang and Zhang, 2016) and the representation of the Indian monsoon (Strømme et al., 2017). Improvements were also found on regime behaviour, northern hemispheric blocking patterns and tropical precipitation (Dawson and Palmer, 2015; Davini et al., 2017; Watson et al., 2017). Most of these studies focused on a particular, multiplicative noise scheme called the ‘stochastically perturbed parametrisation tendencies’ scheme (SPPT). A more flexible variant of this scheme (dubbed ‘ISPT’) was developed and found to substantially improve the skill of weather forecasts in areas with significant convective activity, though only a limited evaluation of its impact on longer timescales was reported (Christensen et al., 2017b). Most modern climate models incorporate also a full land-system and are coupled to an ocean model, both of which carry their own sources of uncertainties. In (Macleod et al., 2016), stochasticity was added to the land-scheme of the IFS, and was found to have a positive impact on seasonal predictability, as well as the 2003 European heatwave. In the ocean, a number of schemes have been considered, including perturbations of ocean mixing processes and sea ice (Juricke et al., 2013; Juricke and Jung, 2014; Juricke et al., 2017, 2018). Both variability and mean-states of key quantities were found to improve. There have more recently also been some studies focusing on the impact of stochastic schemes on the ocean-atmosphere coupling (Williams, 2012; Rackow and Juricke, 2019).

The idea behind the ‘Probabilistic Earth-System’, as put forward in Palmer (2012), is to incorporate stochastic representations of model uncertainty not only into the atmosphere, but also the land, sea ice, and ocean components of the EC-Earth model, thus obtaining a state-of-the-art earth-system model with stochasticity in each major component. Such a fully probabilistic coupled climate model will be tested in the PRIMAVERA project (Haarsma et al., 2016). In this paper, we will present the schemes used in the land and atmosphere components, and perform initial tests in an atmosphere-only configuration. This allows us to test the raw impact of the atmosphere and land schemes on the mean climate with no ocean coupling. In this sense, the study conducted here is a first test of the configurations to be used in the PRIMAVERA simulations. A key motivating question is whether the benefits of such schemes can be achieved without any additional model tuning.

As will be seen, the two atmosphere schemes and one land scheme have a notable impact on the energy budget of the model, implying that in coupled mode, the inclusion of different combinations of these schemes can be expected to shift the model climate to a notably different stable state. In fact, even in these atmosphere-only simulations, we demonstrate significant changes in the mean state of several variables on the large scale, such as atmospheric water vapour content, cloud liquid water, cloud cover, soil temperature and soil moisture. This highlights that the non-linear impacts of random model error, as represented through a zero-mean stochastic perturbation, cannot be neglected in climate models. While some of the changes are positive compared to reanalysis data, not all are. In particular, key global quantities such as net surface energy that models are

35 frequently tuned for, can be strongly altered. This implies that while adding stochasticity can be beneficial, additional model tuning may be required to keep the mean state close to observations.

In section 2, we describe the model used, and the stochastic schemes under consideration. In section 3, we describe the experiments carried out, reference data and statistical methods. Section 4-7 contains the actual analysis. We choose to focus our evaluation on the impact of these stochastic schemes on the mean climate. In sections 4-6, we examine, for each scheme in 5 turn, changes in the global mean of key variables relative to a set of deterministic simulations. These changes provide insight into the impact of the schemes on the energy budget and the hydrological budget. In section 7 we compare changes in the modeled circulation as represented by the Hadley cell and quasi-biennial oscillation (QBO) across all three schemes (SPPT, ISPPT and Stochastic Land). Finally, section 8 contains a discussion on the cause of the observed changes, as well as our conclusions.

10 We note that while we do not test the stochastic ocean schemes here, basic tests of the impact of these on the ocean component NEMO of EC-Earth can be found in Juricke et al. (2017) and Juricke et al. (2018).

## 2 Model Description

### 2.1 About EC-Earth

15 EC-Earth is an Earth system model developed by the international EC-Earth consortium (Hazeleger et al., 2012). The atmospheric component uses a modified version of the Integrated Forecast System (IFS) used by the European Centre for Medium-Range Weather Forecasts (ECMWF). Land-surface processes are simulated using the Hydrology Tiled ECMWF Scheme of Surface Exchanges over Land (H-TESSSEL) (Balsamo et al., 2009). More details are given in section 2.3. Dynamic ocean coupling is available using the Nucleus for European Modelling of the Ocean (NEMO) model version 3.6: as we will consider atmosphere only simulations, we omit further details on the ocean component.

20 The tests in this paper were performed using EC-Earth version 3.2.1, a stable version for atmosphere-only simulations, based on cycle 36r4 of the IFS (released in 2010). The IFS solves the resolved processes in spectral space, with advection and physics parametrisations computed on a reduced Gaussian grid. The parametrizations used are described extensively in (Beljaars, 2004). Modifications to the IFS are carried out to improve the model performance on climate time-scales. In particular, various parameters controlling the physics parametrizations were tuned by the consortium to obtain a realistic energy budget in the 25 period 1990-2010, as compared to observational estimates (Trenberth et al., 2009).

In all experiments carried out, we used the default resolution of the current EC-Earth version, which uses 91 vertical levels and a spectral resolution of T255, corresponding to a horizontal resolution of around 80 kilometres.

### 2.2 Description of the SPPT and ISPPT schemes

The SPPT scheme has been included in the operational model of the IFS since 1998. The scheme is designed to represent forecast uncertainty that arises from the simplifications and approximations involved in the parametrisation of unresolved

atmospheric processes. It does this by perturbing, at each timestep, the total net tendency from the physics parametrisations using a multiplicative noise term  $r$ :

$$\hat{\mathbf{P}}_{\mathbf{k}} = (1 + \mu_k r) \sum_{i=1}^6 \mathbf{P}_{i,k}, \quad (1)$$

- 5 where  $\mathbf{P}_{i,k}$  is the vector made up of the tendencies of the prognostic model variables (winds, temperature and humidity) from the  $i$ -th physics parametrisation scheme, where  $k$  indicates the vertical model level. The physics schemes are as follows: 1st=radiation (RDTN), 2nd=turbulence, vertical mixing and orographic drag (TGWD), 3rd=convection (CONV), 4th=large scale water (cloud) processes (LSWP), 5th=non-orographic drag (NOGW), and 6th=methane oxidation (MOXI). The perturbation,  $r$ , is constant in the vertical, but is tapered through  $\mu_k \in [0, 1]$  to smoothly reduce the perturbation to zero in the
- 10 boundary layer and stratosphere; this is done to avoid introducing numerical instabilities. The perturbation  $r$ , which evolves in time, follows a Gaussian distribution with mean zero, and is smoothly correlated in space and time. The implementation in EC-Earth follows that in the Integrated Forecasting System as described in (Palmer et al., 2009). The perturbation  $r$  is generated by summing over three independent spectral patterns with standard deviations (0.52, 0.18, 0.06), spatial correlation lengths (500 km, 1000 km, 2000 km) and temporal decorrelation scales (6 hours, 3 days, 30 days) respectively: the different patterns are
- 15 meant to capture model error at different scales which may, in principle, be independent of each other. The perturbation  $r$  is limited between -1 and 1 to ensure  $\hat{\mathbf{P}}$  has the same sign as  $\mathbf{P} = \sum \mathbf{P}_i$ .

- The SPPT scheme described above assumes that the different physics parametrisations have the same model error characteristics. If the net tendency is small, SPPT represents the associated model uncertainty as small, even if the associated individual tendencies were large. (Christensen et al., 2017b) proposed a generalisation to the SPPT approach in which each physics
- 20 process is perturbed independently using multiplicative noise:

$$\hat{\mathbf{P}} = \sum_{i=1}^6 (1 + \mu_k r_i) \mathbf{P}_{i,k}, \quad (2)$$

- The random patterns,  $r_i$ , are independently generated and evolved. The statistical properties of the  $r_i$  (standard deviation, spatial and temporal correlations) can be individually specified to account for differences in the uncertainty characteristics arising from each physics scheme. This generalisation, ‘Independent SPPT’ (ISPPT), was shown to significantly improve the
- 25 reliability of ensemble forecasts in the tropics, and in areas with significant convective activity (Christensen et al., 2017b). This indicates ISPPT is likely a better representation of the uncertainty associated with convection than SPPT. Further justification for the use of ISPPT over SPPT has been provided by considering coarse-graining experiments (Christensen, 2018).

- Note that in these standard implementations of SPPT and ISPPT, the fluxes in precipitation and evaporation are not perturbed using the random pattern. Implementing such a change would improve consistency in the transport of moisture in the model,
- 30 and is of interest for future investigation.

Finally, it has been found, in Davini et al. (2017), that the SPPT scheme does not conserve water, leading to an unphysical drying of the atmosphere. A ‘humidity fix’ was introduced in *ibid*, which we also use for our SPPT and ISPPT experiments. The ‘fix’ computes, at each time-step, global mean precipitation and evaporation, and reinserts the amount of humidity required to bring these into balance. This humidity is reinserted with spatial weighting favouring regions where the imbalance is large.

### 2.3 Description of the Stochastic Land scheme

The land surface model used here is H-TESEL, the Tiled ECMWF Scheme for Surface Exchanges over Land (TESSEL) with revised land surface hydrology, comprising a surface tiling scheme and vertically discretized soil. The surface tiling scheme allows each gridbox a time-varying fractional cover of up to six tiles over land (bare ground, low and high vegetation, intercepted water, and shaded and exposed snow) and two over water (open and frozen water). Each tile has a separate energy and water balance, which is solved and then combined to give a total tendency for the gridbox, weighted by the fractional cover. Full details of the model may be found in Balsamo et al. (2009).

Stochasticity is induced in the land-scheme via the hydraulic conductivity, which is calculated in H-TESEL using the van Genuchten formulation (van Genuchten, 1980). This formulation is favoured by soil scientists as it has shown good agreement with observations in intercomparison studies (Shao and Irannejad, 1999). The hydraulic conductivity is in this formulation given by

$$\gamma = \gamma_{sat} \frac{[(1 + \alpha h^n)^{1-1/n} - \alpha h^{n-1}]^2}{(1 + \alpha h^n)^{(1-1/n)(l+2)}}, \quad (3)$$

where  $\alpha$ ,  $l$  and  $n$  are soil texture parameters, dependent on the soil type,  $h$  is soil water potential (the potential energy of soil water due to hydrostatic pressure), and  $\gamma_{sat}$  the hydraulic conductivity at saturation. The two key soil parameters  $\alpha$  and  $\gamma_{sat}$  of Eq. 3 are stochastically perturbed. These particular parameters have been chosen as previous studies found them to be particularly sensitive (Cloke et al., 2008; MacLeod et al., 2016). Each parameter is perturbed with its own integration of the spectral pattern generator. As with SPPT and ISPPT, the spectral pattern is obtained as a sum of three patterns, each with the same spatial and temporal decorrelation scales as for those schemes. The weightings for each scale is in this case set to 0.33. Estimates of these parameters based on observational data suggests that the two parameters are correlated (Cosby et al., 1984) and so a third pattern is used as a base for each pattern, in order to introduce correlation between them. The correlation coefficient between the two parameters is prescribed to be 0.6 on average. The perturbation is multiplicative, as with SPPT. That is, each parameter  $p$  is multiplied by  $(1 + r)$  where  $r$  is the randomly generated spectral pattern described above.

Previous work has investigated the impact of representing uncertainty in these particular hydrology parameters. Perturbing coupled atmosphere-ocean seasonal hindcast experiments (MacLeod et al., 2016) resulted in an improved representation of soil-moisture driven processes active during the 2003 heatwave, leading to an improved signal in the seasonal forecast of surface air temperature. In a set of atmosphere-only experiments, MacLeod et al. (2016) showed a strong sensitivity of soil moisture memory to uncertainty in these parameters. Using the same atmosphere-only model, Orth et al. (2016) also demonstrate an improvement in subseasonal forecast skill through incorporation of land surface parameter uncertainty.

## 3 Data and Methods

### 3.1 Experimental setup and reference data

We performed four ensemble experiments, which we will for brevity refer to as CTRL, SPPT, ISPPT and LAND, referring to the scheme being used in each (in the CTRL experiments no stochastic schemes were used). The ensemble members were run for 20 years each, starting from February 1st of the following years: 1960, 1965, 1970, 1975, 1980. Thus the total period covered by all the experiments is 1960-2000. The motivation for spacing out the members in this way was to account for the possibility that the impact of the schemes may be sensitive to the initial ocean state. The creation of an ensemble, as opposed to e.g. a single, longer run, was motivated by the experience from ensemble forecasting using stochastic schemes, where multiple ensemble members are typically needed to estimate changes robustly. While spin-up issues may have been a complicating factor in these shorter experiments (especially for the LAND simulations, given the slow variations in soil moisture), initial testing suggested that the model adjustment was rapid, further justifying the use of an ensemble of shorter runs.

Atmospheric initial conditions for these dates were provided by the Climate Prediction group at the Barcelona Supercomputing Center. These initial condition files are obtained by interpolation of reanalysis data using the FULLPOS post-processing software for the IFS: this carries out the interpolation using the model executable to ensure minimal model drift (Bellprat et al., 2016). The sea surface temperatures and sea-ice are then specified using the CMIP6 forcing datasets to match observations. Radiative forcings such as those from anthropogenic or volcanic sources were provided by the same source.

For the SPPT scheme, we used the default settings for the magnitudes and time/length-scales of the perturbations as in (Leutbecher et al., 2017), described in section 2.2.

For ISPPT, we used the same settings for the 3 fields as for SPPT. We set the convection and large-scale water-process tendencies to share the same perturbation, and let the remaining four tendencies (radiation, turbulence and gravity wave-drag and non-orographic gravity wave drag) have separate, independent perturbations. We chose to use the same perturbation because of the feedbacks between the convection and large-scale water processes schemes in the IFS, whereby detained moisture from the convection scheme acts as an input to the large-scale water processes scheme. Perturbing the two schemes together therefore improves consistency of moisture transport in the model. Following the naming convention introduced in Christensen et al. (2017a), this corresponds to ISPPT 1,2,3,3,4,5, where the number indicates which random seed was used to generate a pattern and the ordering of the numbers indicates which of the 6 physics parametrisation schemes are perturbed with that pattern (see section 2.2).

For the LAND scheme, the parameter perturbations  $r$  were restricted to be strictly between 1 and -1, as numbers greater than or equal to 1 were found to produce unphysical runoff behaviour. For this reason, the standard deviation of the noise perturbations were set to 0.33, allowing three standard deviations to explore the full available range.

To allow for a single reanalysis dataset to be used across all the experiments, ERA40 (Uppala et al., 2005) was chosen as our reference point. When evaluating the QBO, we use the more recent reanalysis dataset ERA-Interim (Dee et al., 2011). A disclaimer here is that these reanalysis datasets are both created via data assimilation using previous versions of the IFS, and are hence in some ways related to EC-Earth. For variables that are less strongly constrained by the assimilation of existing observations (such as total cloud cover), this may imply that the model bias may not be independent of any existing biases within the reanalysis data themselves.

Finally, we note that additional simulations were also performed with both SPPT+LAND and ISPPT+LAND configurations, to test the combined impact of schemes. However, it was found that the impact of SPPT/ISPPT dominates the impact of LAND when it comes to the large-scale changes considered in this paper. Therefore, we have omitted these configurations in the present paper.

### 3.2 Methodology

### 3.3 Statistical Techniques

All fields considered were filtered by taking monthly means. To compute the mean impact of the scheme, each simulation is paired with the corresponding CTRL simulation covering the same time period. The difference of each individual pair is computed, and the mean across the five ensemble pairs gives the mean impact of the scheme. When comparing the CTRL simulations with reanalysis, each CTRL simulation is paired with the reanalysis data for the corresponding time-period, and again the mean across all five pairs defines the CTRL bias. The standard deviation across the five ensemble members is used to estimate the statistical significance of the mean differences between model simulations. Twice the standard deviations is used as an error bound (displayed either with shading in time-series plots or explicitly written as a number in percentage change plots). Because there are only five samples, it is hard to claim that differences are definitively significant even if the zero-line is further than two standard deviations away from the mean. However, in the cases where this does happen, we have observed that all five individual differences have the same sign, suggesting that in these cases the difference is likely significant.

To assess differences in spatial patterns, the five ensemble members are concatenated to produce a timeseries spanning 1200 months at each grid point for each simulation, with the ensemble members ordered according to their start date. A two-tailed T-test is applied to assess the significance of the difference in the mean. Spatial plots then indicate the mean difference across all the five simulations. Gridpoints where the difference lies outside the 95% confidence interval are marked with dots. A cruder test was also used which simply tested if four of the five differences had the same sign. The results were almost identical.

Finally, to assess whether a reduction in the mean-square error (MSE), relative to re-analysis, was significant, we computed the MSE for all five simulations of the scheme in question, as well as the five MSE's of the CTRL simulations. If the difference between the mean CTRL MSE and the mean MSE of the scheme was greater than two standard deviations of the spread in MSE's across the five scheme simulations, the difference was deemed significant.

### 3.4 Energy Budget

As the simulations were performed with historical forcings, the energy budgets of the five CTRL simulations are not comparable with each other. However, since the EC-Earth Consortium tuned the deterministic model to have a realistic energy budget over the period 1991-2010, the surface fluxes of the CTRL simulation covering the period 1991-2000 are shown in Table 1. The table has been split into two parts, as the Pinatubo eruption in 1991 has a strong influence on the first half of the period. For reference, the estimates of these quantities from (Trenberth et al., 2009) (covering 2000-2004) are also shown.

It can be seen that the CTRL simulation achieves a reasonable energy balance, with the net surface energy close to the observational estimate. As will be seen, the adjustment to this budget by the introduction of the different stochastic schemes is very fast and approximately constant in time. Therefore, it is possible to assess whether the stochastic schemes lead to an improved or degraded energy budget overall, though it should be kept in mind that variations in the budget between years is often large. **Focusing the comparison against observations to this particular timeperiod ignores possible changes to the evolution of the surface energy fluxes over time, i.e. possible changes in the climate sensitivity of the model. As this is the topic of the forthcoming study ?, we do not consider this in the present manuscript.**

## 4 The impact of SPPT

### 10 4.1 Impact on mean state

Figure 1(a) shows the percentage changes in global mean quantities due to SPPT, relative to the CTRL simulation. Evaporation has notably increased by about 1%. Figure 2(b) shows the spatial distribution of these changes<sup>1</sup> averaged across all seasons, to be compared against the bias of the CTRL simulations to reanalysis, Fig. 2(a). The increase can be seen to be concentrated in the western Pacific oceans in particular, with a notable decrease in the eastern Pacific. We note that the spatial changes due to SPPT are not well correlated with the CTRL bias, reducing the bias in places and exacerbating it elsewhere. As the overall mean CTRL bias is close to 0, the net increase in evaporation due to SPPT represents a small degradation. This is also reflected in the mean-square error (MSE) between the spatial means of SPPT and reanalysis, as found in Table 2, where it can be seen that the MSE has increased with SPPT.

By contrast, precipitation, as seen in Fig. 3(b), has generally improved. This can be seen both in terms of the mean bias, which has approximately halved, and the MSE (Table 2). While the precipitation biases of the CTRL model (plot (a) of the same figure) are targeted well in key areas, such as the Pacific and Indian oceans, the scheme exacerbates the biases elsewhere, such as over the maritime continent and in sub-Saharan Africa.

**The scheme has also notably affected clouds, with cloud cover decreasing at all levels and cloud liquid water (the vertical integral of liquid water contained within clouds in a gridpoint column) robustly increasing. Figure 4(b) shows the spatial distribution of total cloud cover changes. The spatial pattern of cloud liquid water changes (not shown) are well correlated with these cloud cover changes, suggesting that while cloud cover in total has gone down, the remaining clouds are more optically thick. Note that because cloud cover has decreased, the actual increase in cloud water due to SPPT is likely proportionally larger than the 1.2% measured.** Comparing Fig. 4(a) and (b) also shows that the net impact of SPPT on total cloud cover is to significantly reduce the CTRL bias. Indeed, SPPT has almost uniformly reduced the bias everywhere, bringing the mean bias down to nearly 0. The MSE has also gone down by about 15%.

The impact on the spatial biases of two meter temperature across all seasons are also shown in Fig. 5(b). The cold bias in the CTRL simulations (plot (a) of the same figure) across the equator can be seen to be robustly decreased by SPPT. The

---

<sup>1</sup>Note that we have not adhered to the IFS convention here that downward fluxes are positive. Thus red values indicate an increase in evaporation *upwards*.

statistically significant increase in temperatures over sub-Saharan Africa is on the other hand introducing a bias that was not present in the CTRL model. No notable impact is made on the warm bias in the Arctic and Antarctic regions, and there is no notable change in the MSE overall, nor the total mean bias.

## 4.2 Impact on energy budget

Figure 6(a) shows the mean difference between each SPPT-simulation with the corresponding CTRL-simulation for the globally averaged surface energy fluxes shown in 1. Note that the standard EC-Earth convention has been used whereby downward fluxes are positive. Hence, a positive difference for a given flux indicates that the scheme increased the flux in the downwards direction on average, while a negative difference indicates an increase in the upwards direction on average. The benefit of adhering to this convention is that the net surface energy, always in black, can be obtained by summing up all the other flux-quantities in the plots. In this way, it is easy to assess which quantity is having the strongest influence on altering the net budget. The timeseries have also been smoothed by a 12-month running mean both to remove both the seasonal cycle and to highlight the overall trends.

It can be seen that the dominant impact of SPPT is a large increase in latent heat flux consistent with the strongly increased evaporation identified in the previous section. This in turn is the main contribution to the reduced net surface energy, with the total mean difference being  $-0.8 \text{ W/m}^2$ . Compared to the baseline budget from Table 1, this clearly represents an unrealistic reduction in surface energy.

There is also a notable increase in surface solar radiation (SSR). The previous section indicated that, while cloud liquid water increased by around 1.2%, the total cloud cover decreased at all levels through the atmosphere. Thus it appears that while the clouds are more optically thick, which would tend to decrease SSR, the reduction in cloud cover leads to an overall increase in shortwave radiation reaching the surface.

Finally, note that because the difference is essentially constant in time, we can infer two important points. Firstly, the impact of the scheme on the energy budget is independent of the initial ocean state, and secondly, the scheme does not lead to any systematic drift: the model fully adjusts to the scheme within 1 month.

## 4.3 Impact on the hydrological budget

Figure 7(a) shows the percentage changes in the total column soil water content (SWVLTOT) along with the three quantities responsible for modulating this quantity: precipitation, evaporation and total runoff. Note that precipitation and evaporation here have been restricted to land-points only, explaining why the numbers do not exactly match those of Fig. 1(a). There is a small but significant decrease in the total soil water of around 1%. As the SPPT scheme only directly interacts with atmospheric processes, this change will be driven by the observed changes in precipitation and evaporation. Over land, precipitation decreases by around 1.7% and evaporation increases by about 1%, both of which contribute to the decrease in soil water. The notable decrease in runoff is likely a consequence of the reduction in water in the soil column. By reference to Table 2, the runoff changes, seen in Fig. 8(b) are beneficial overall, reducing the MSE.

## 5 The impact of ISPPT

### 5.1 Impact on mean state

Figure 1(b) shows the percentage changes in global means induced by the ISPPT scheme. The signal of increased evaporation and cloud liquid water seen with SPPT is greatly amplified. Figure 2(c) shows the spatial distribution of evaporation changes, which as with SPPT are strongest over the tropical oceans. The total increase in evaporation is even greater than that from SPPT, and again represents an overall increase in the global mean bias. However, there is an enhanced spatial coherence between the local changes from ISPPT and the CTRL bias (plot (a) of the same figure). It can be seen that the sign of the ISPPT changes are generally opposite to the sign of the CTRL bias, indicating that the scheme is effectively targeting the local biases, with a notable exception being the ocean region south of Australia. This is reflected in the fact that while the global mean bias has increased, the MSE (Table 2) has decreased.

Figure 3(c) shows the changes in precipitation. Again, local biases are well targeted, with the MSE decreasing even more than with SPPT. The mean bias relative to reanalysis has been reduced to near 0.

Unlike SPPT, total cloud cover has only decreased by a very small amount, due entirely to a decrease in the high level clouds which dominates a small increase in low and mid-level clouds. Figure 4(c) shows the change in total cloud cover, where areas of overall decrease indicate decreases in high level cloud cover. As with SPPT, the changes serve to decrease the CTRL bias, both in total and locally, as can be seen by a notable decrease in the MSE (Table 2). Interestingly, there is great spatial coherence between these changes and those seen for SPPT in Fig. 4(b). Indeed, an examination of these and other variables generally suggests that a first-order approximation of the *mean* impact of ISPPT is a stronger amplitude version of the impact of SPPT, but with the changes being even more closely correlated with the local biases, as seen with evaporation and precipitation above. The added freedom of non-correlated perturbations with ISPPT allows for a stronger influence on non-linear climate processes, most notably those associated with convective processes (Christensen et al., 2017b).

Figure 5(c) shows the local changes in two meter temperature. As with SPPT, the cold bias along the equator is reduced, but unlike SPPT, the warm biases in the Arctic and Antarctic regions are also reduced. The globally averaged mean bias has been reduced by nearly 70%, and the MSE has decreased by nearly 25%.

### 5.2 Impact on energy budget

Figure 6(b) shows the flux impact of ISPPT. As with SPPT, the dominant effect is from the substantial increase in evaporation, as seen in Fig. 2(c). In contrast to SPPT, ISPPT also results in a substantial reduction in SSR of almost  $1 \text{ W/m}^2$ . Figure 1(b) shows that while there was a small decrease in total cloud cover, low level cloud cover (the layer reflecting the most solar radiation), has increased by around 0.5%. Even more notably, the cloud liquid water content has increased by nearly 5%, increasing the albedo of these clouds significantly. These factors combine to explain the decreased SSR. A mild increase in sensible heat flux and thermal radiation cannot compensate this, such that the net result is a large decrease in surface energy of around  $1.7 \text{ W/m}^2$  relative to CTRL. By reference to Table 1, this represents a large divergence from observed values.

As with SPPT, the impact of the scheme is effectively constant in time, and therefore independent of the underlying initial ocean state.

### 5.3 Impact on hydrological budget

10 Figure 7(b) shows percentage changes for the hydrological budget for the ISPPT scheme. There is no notable change in precipitation over land, but evaporation has increased by around 3%. This will have a drying effect on the top soil layer. Despite this, no meaningful change is seen in the total column soil water. One possible explanation for this is to first note that in general, if the top soil layer holds more water, heavy rainfall events will tend to saturate the surface, triggering the land-scheme to expel a lot of this water as runoff already at the top soil layer. This will tend to inhibit moisture from sinking  
15 down to the lower soil layers. Conversely, if the top layer is drier, as seen with ISPPT (due to e.g. the increased evaporation), runoff at the top soil layer will not be triggered as easily during rainfall, allowing more water to reach the lower layers. In this way, increased evaporation can be balanced by reduced runoff to produce no overall change in total soil water. Noting the reduced runoff in Fig. 7(b), seen visually in Fig. 8(c), we speculate that this is the reason there is no change in soil water due to ISPPT. **Of relevance to this is the fact that more frequent heavy rainfall events may be expected with ISPPT, as this is the case  
20 with SPPT ((Watson et al., 2017)): this could easily trigger the above mechanism.**

We finally note that by Table 2, the runoff changes are broadly beneficial, reducing the MSE even more than SPPT does.

## 6 The impact of Stochastic Land on the mean state

### 6.1 Impact on basic mean state

Figure 1(c) shows the percentage changes in global means induced by LAND. As with both SPPT and ISPPT, evaporation  
25 increases. Spatial changes here are shown in Fig. 2(d), where visual inspection shows that the changes mostly serve to reduce the CTRL bias (plot (a) of the same figure). This is confirmed by a reduction in MSE, as seen in Table 2. As we will see in the section on hydrology, the changes in evaporation over land are strongly correlated with changes in runoff. Since evaporation changes over land can have knock-on effects on the global circulation more broadly, this already suggests a mechanism whereby the LAND scheme, which only directly interacts with soil processes, can still lead to global mean state changes.

30 For precipitation, seen in Fig. 3(d) and Table 2, while the MSE has gone down compared to the CTRL runs, the mean bias remains unchanged. While the precipitation bias over the Indian ocean and maritime continent are decreased, biases over India are increased and the changes over the Pacific ocean are fairly ambiguous in their merit.

Unlike SPPT and ISPPT, the LAND scheme has a more notable impact on total column water, increasing it by nearly 1%. The cloud cover changes are similar in characteristic to those of ISPPT, with low and mid-level cloud cover increasing, and  
5 high level cloud cover decreasing: Fig. 4(d) shows the spatial distribution of these changes. It can be seen that while the LAND scheme has reduced biases over all the major continents (with the exception of Australia), as well as over the Indian Ocean, it

has had only a limited impact over the Pacific and Atlantic ocean. Consequently, the MSE, recorded in Table 2 has not changed relative to CTRL.

Figure 5(d) shows the spatial changes in two meter temperature, where the major, statistically robust change is a big reduction in the warm bias in the Arctic and Antarctic regions. This has reduced the overall mean bias relative to reanalysis by around 90%, as well as notably reducing the MSE.

## 6.2 Impact on the energy budget

Turning on the LAND scheme has only a small impact on the energy budget (Fig. 6(c)), increasing net surface energy by about  $0.1 W/m^2$  relative to CTRL. The primary culprit appears to be a decrease in outgoing longwave radiation. Figure 1(c) shows that atmospheric water vapour has increased by about 1%, which would, by strengthening the greenhouse effect, serve to trap more thermal radiation in the atmosphere. While the same figure shows high level cloud cover has decreased, which would tend to negate that effect, the large increase in mid level cloud cover may counteract the change in high level cloud to a large degree, such that the water vapour increase ends up being the dominant driver of energy budget changes.

As with SPPT and ISPPT, the impact of the scheme is effectively constant in time, and therefore independent of the underlying initial ocean state.

## 6.3 Impact on the hydrological budget

Figure 7(c) shows the percentage changes observed on including the LAND scheme, restricted to land-points only. The scheme has a big impact on both runoff and soil moisture over Antarctica. However, the run-off scheme is typically not behaving realistically here, where the soil is trapped under thick layers of ice. To avoid the quantified impacts being dramatically skewed from this contribution, we excluded Antarctica from the data prior to computing percentage changes<sup>2</sup>.

Firstly, it can be seen that there is no statistically robust change to the overall soil water content. This is puzzling at first sight, since it can also be seen that there is an increase of precipitation over land which is not canceled out by an equal amount of evaporation; runoff has also decreased robustly by around 1%. These changes would be expected to lead to an increase in soil water. Indeed, examining the spatial distribution of soil water changes (not shown), one finds that areas of increased precipitation (Fig. 3(d)) do mostly correspond to areas of increased soil water content, and vice versa. The two main exceptions are over Greenland and Siberia, where a behaviour similar to that seen in Antarctica is observed (strongly decreased soil water and runoff) even with no meaningful change in precipitation. Figure 8(d) shows the spatial distribution of runoff changes. The areas of increased runoff correlate well with areas of increased precipitation/soil water content, with runoff triggered more frequently the wetter the soil. The exceptions of Greenland and Siberia are clearly visible.

This suggests that in regions not dominated by ice and snow, long-term changes in runoff and soil water are driven by the long-term circulation changes induced when stochastically perturbing hydraulic conductivity. However, in regions such as Siberia and Greenland, there is a sharp decrease in soil water content within the first month of each LAND simulation, with

---

<sup>2</sup>Note that this was not done for the other schemes, where quantities computed globally also included Antarctica.

no associated change in surface evaporation. This extra decrease in soil water, independent of precipitation and evaporation changes, explains why the total soil water mean has not changed overall.

Comparing the runoff impacts with the CTRL bias (plot (a) and (d) of Fig. 8), we see that the local biases have mostly  
10 been improved, with the MSE (Table 2) decreasing by about 10%, suggesting the increased variability in the LAND scheme is serving to reduce the model bias.

## 7 Impact on atmospheric circulation

We now assess the impact of all three schemes on two key components of the atmospheric circulation: the Hadley Cell and the quasi-biennial oscillation (QBO). Our examination of the former is motivated by the fact that, as we have seen in the  
15 above sections, the schemes tend to have a large impact on tropical convection, hinting at possible changes in the Hadley Cell circulation. The motivation for examining the latter comes from an earlier study, Leutbecher et al. (2017), on the impact of the SPPT scheme on the IFS in shorter range forecasts. It was found in *ibid* that the most notable degradation of the scheme on the model was in the upper level winds, where the QBO dominates variability. This was noted as a potential source of concern, as literature suggests the QBO influences the extra-tropical winter climate. Table 2 shows the MSE of zonal winds at  
20 various levels: in agreement with *ibid*, we see a large increase in the bias at the 10hPa level. We therefore explicitly examine the performance of the QBO in our experiments to assess the possible changes.

### 7.1 Impact on the Hadley Cell

The impact of the stochastic perturbations on the atmospheric circulation is considered through analysis of the Hadley circulation. The Hadley cell varies with the seasonal cycle, and is stronger and wider in the winter hemisphere: we consider the  
25 characteristics of the dominant Hadley cell separately for the key seasons December/ January/ February (DJF) and June/ July/ August (JJA). We characterise the zonally-averaged overturning circulation using a streamfunction,  $\psi$ , defined as a function of latitude and height, following Waliser et al. (1999). The procedure is performed separately for each simulation.

To consider the effect of stochastic physics, we calculate three summary diagnostics for the cell. Firstly, the strength of the overturning is characterised using the maximum of the streamfunction. The width of the overturning cell is indicated by  
30 estimating the latitude of the upwelling and downwelling branches of the cell respectively. This is defined as the latitude at which the streamfunction changes sign at the 700 hPa level. The 700 hPa level was chosen as this corresponds to the approximate level at which the streamfunction maximum is found. These results are shown for each ensemble member in Fig. 9 by the five scattered points. The diagnostics are also shown for ERA40 for the five time periods corresponding to the five ensemble members.

Panels (a) and (b) show the strength of the overturning circulation for each simulation and both seasons. The SPPT scheme  
5 shows no significant impact on the strength of the overturning in DJF, and a slight though not significant weakening in JJA. In contrast, both the ISPPT and LAND approaches show a significant strengthening of the overturning cell in both DJF and JJA.

For all simulations, the JJA cell is stronger than the DJF cell. While the CTRL and SPPT simulations have a somewhat too weak Hadley cell, the Hadley cell in the ISPPT and LAND experiments is too strong.

Figure 9 (c) and (d) show the latitude of the downwelling branch of the dominant cell for each season. As for the strength of the circulation, SPPT has no significant impact on this diagnostic. Both the ISPPT and LAND schemes lead to a significant equator-ward shift of the downwelling latitude in DJF, in contrast to what is seen in reanalysis. In JJA all simulations are in agreement with ERA40, and only the LAND scheme leads to a slight equatorward shift.

Panels (e) and (f) show the latitude of the upwelling branch of the circulation. SPPT leads to no significant change in this diagnostic, while the ISPPT and LAND schemes lead to a large shift poleward. This introduces a substantial bias when compared to ERA40, which needs to be understood. The net effect of this is to increase the width of the Hadley circulation in the ISPPT and LAND simulations.

The Hadley circulation is changing in response to climate change. There is evidence that it has widened over recent decades (Hu and Fu, 2007; Seidel and Randel, 2007), and some evidence that it has also strengthened (Seager et al., 2007), though GCMs struggle to reproduce the observational signal (Mitas and Clement, 2005; Johanson and Fu, 2009). To compare the climate change impact on the Hadley circulation for each stochastic model, we indicate the years covered by each simulation in Fig. 9.

The deterministic simulations show a general strengthening of the DJF Hadley circulation, though a weakening of the JJA Hadley circulation. This trend is also observed in DJF for the three stochastic models, though the signal in JJA is more mixed. While there is no climate change signal observed in the latitude of the downwelling branch for any simulation, the simulations generally agree that the DJF upwelling branch has shifted poleward. The exception is the ISPPT simulation, which does not show a strong sensitivity in this diagnostic.

## 7.2 Impact on the quasi-biennial oscillation

The QBO is a periodic downward propagation of easterly and westerly wind regimes which accounts for the majority of variability in the equatorial stratosphere (Baldwin et al., 2001), exerting a notable influence also on the extratropical atmosphere through modulating extratropical waves. Its period is typically estimated to be around 28 months.

Figure 10 shows the average QBO period across each simulation for each of the four experimental set-ups, as well as that for ERA-Interim. For each scheme, the period marked with a cross in the figure is the average period across the five ensemble members; the errorbar shows two standard errors of this mean estimate. The period was here diagnosed using zonal equatorial (10S-10N) winds at 50hPa, zonally averaged. This produces a periodic timeseries from which we can readily estimate the average spacing between zero-crossings to determine the average period. When applied to the reanalysis dataset ERA-Interim, this produces a period of almost exactly 28 months, suggesting that this method captures the expected period well. It can be seen that the deterministic model itself cannot achieve nearly as long a period, falling just below 21 months. Both SPPT and ISPPT have reduced the period by a small amount, but compared to the initial bias of the deterministic model itself these changes are small. While the mean period of LAND is slightly smaller than CTRL, the errorbars are large enough to imply that this decrease is not statistically robust.

Figure 11 shows a time-pressure level section of monthly averaged zonal wind, restricted to the equatorial region 10S-10N with the seasonal mean removed. This gives the usual visual representation of the QBO for the ensemble members covering the 1980-2000 period, with ERA-Interim over the same period also shown: the behaviour of these members are representative of the full ensemble, where there is little year to year variability in the degradation of the QBO. It can be seen that indeed EC-Earth struggles to attain both a strength, period, and extent of downwelling comparable to ERA-Interim. None of the stochastic schemes notably change this; in particular, there is no notable additional degradation compared to the CTRL simulation.

## 8 Discussion and Conclusions

### 8.1 Discussion

Because the impact of the schemes appears to be firmly in place within the first month of each experiment, a comprehensive study pinning down the cause of the observed changes would require a more process-based investigation of the rapid response. As the experiments considered in this manuscript were constructed to examine long-term rather than rapid changes, such an investigation will be left to future work. However, for completeness, we include some discussion here on what the key processes at play may be. We note that an examination of the rapid response of EC-Earth to SPPT was carried out in ?. Analysis in this paper shows that the most robust, rapid change when turning on SPPT is an increase in cloud liquid water and evaporation, thereby largely supporting the arguments presented in what follows.

With both SPPT and ISPPT, the dominant impact on the energy budget is increased evaporation. In the IFS, the amount of evaporation at a gridpoint depends primarily on the surface wind-speeds and the extent to which the specific humidity at the surface gridpoint differs from the saturation humidity (a function of surface temperature). While wind-speeds do increase by about 1.4% on average with ISPPT, the mean wind-speeds are unchanged with SPPT, with a tiny increase of only 0.06%. Given that the increase in evaporation of both SPPT and ISPPT are of the same order of magnitude, this suggests changes in humidity are a key factor. Because SST's are held fixed, such changes will be, to first order, driven by changes in the water content of the atmosphere as opposed to temperature changes at the surface. One possibility is that the increase in cloud liquid water is depleting the near-surface humidity, causing more favourable conditions for evaporation. The fact that both cloud liquid water and surface wind-speeds increase more with ISPPT could then explain why this impact is amplified in those experiments. Another possibility is that the first order impact is on convection in the tropics, which may be activated more frequently with SPPT/ISPPT. This could lead to a drying of the boundary layer, promoting more evaporation in response.

Furthermore, the increase in cloud liquid water with both SPPT and ISPPT could be due to an asymmetric response to stochastic perturbations in the convection schemes. Given a parcel of air close to saturation, whether the model actually triggers condensation depends sensitively on the humidity and temperature tendencies, both of which are perturbed by the stochastic schemes. A perturbation in one direction may result in condensation, and thereby an increase in the cloud liquid water, while a perturbation in the other direction leaves the parcel stable and the total cloud liquid water unchanged. Since the stochastic perturbations are zero mean, it is expected that these two scenarios will occur at the same rate, such that the net impact of the perturbations is to increase the total amount of cloud liquid water, as observed. An important point here is that the SPPT/ISPPT

scheme has a ‘supersaturation limiter’ in place (Palmer, 2012). This limiter essentially ensures that any perturbations which would result in a parcel of air being pushed into a supersaturated state are ignored. The mechanism described above therefore cannot be taking place within a single timestep. However, never the less, a perturbation may still push a parcel of air closer to saturation, whereby the model dynamics themselves may bring the parcel towards condensation on the subsequent timestep. In this way, SPPT/ISPPT, by generally broadening the distribution of temperature/humidity tendencies, may lead to increased condensation on average.

We suggest that the changes in evaporation/convection and cloud liquid water are the main sources of large-scale changes to the mean climate caused by SPPT and ISPPT. These variables strongly control cloud formation, cloud albedo and latent heat release, which are the dominant sources of changes to the energy budget.

In addition, changes to evaporation (and thereby precipitation) dominate the hydrological budget. Since the atmospheric circulation is also coupled to thermodynamic processes, especially in the tropics, it is likely that the observed impact on the Hadley cell can also be traced to these changes in the hydrological cycle. This is supported by Numaguti (1993), which showed that the strength and meridional structure of the Hadley cell is closely linked to the distribution of evaporation. With both ISPPT and LAND the change in the Hadley cell is largely detrimental compared to reanalysis, implying that some of the positive impacts seen on the mean state may be due to a compensation of errors. This would need to be studied more carefully in future work.

For the LAND scheme, the first-order impact appears to be regional changes in average runoff. That such changes should be expected to occur can be understood by reference to Eq. (3) defining hydraulic conductivity. Because runoff is triggered when the soil becomes saturated, its triggering is intimately linked to the ratio  $\gamma/\gamma_{sat}$ , which reaches its maximum of 1 precisely at saturation. This ratio, as seen in Eq. (3), is highly non-linear in the perturbed parameter  $\alpha$ , implying that even mean-zero perturbations can be expected to alter the mean state. This will lead to regional changes in the moisture content of the soil layer, which in turn influences evaporation over land. The net impact is a decrease in runoff and therefore an increase in evaporation. This change permeates through to influence the rest of the climate system, including an increase in total column water and large changes in the vertical distribution of cloud coverage.

## 8.2 Conclusions

Three stochastic schemes are introduced into the atmosphere and land components of the EC-Earth climate model. The stochastic schemes incorporate zero-mean perturbations into the model physics to represent uncertainty associated with unresolved, sub-grid scale variability. The interaction of these perturbations with the non-linear Earth-system results in systematic changes to the mean state of the model in a way that is not a priori obvious. Schemes that are fairly similar (SPPT and ISPPT) may have very different impacts, and schemes that are only directly affecting a relatively small component of the model (LAND) may still notably change the global circulation. This highlights the importance of representing random model error in climate models, as well as in initialised simulations, where stochastic schemes have long been used to improve the reliability of forecasts (Palmer et al., 2009; Berner et al., 2017).

Our experiments showed that the inclusion of all three stochastic schemes, particularly ISPPT and LAND, led to notable reductions in model biases compared to the deterministic model. This is seen perhaps most strikingly for two-meter temperature, precipitation and total cloud cover, three important quantities where both the mean bias and the MSE were reduced. The distribution of runoff, a key driver of land-atmosphere interaction in EC-Earth, was also improved by all three schemes. This demonstrates that the inclusion of stochastic schemes can have a beneficial impact on a models long-term climate mean state.

On the other hand, none of the schemes are able to improve the representation of the QBO, and the Hadley cell becomes too strong and widens too far polewards with ISPPT and LAND. This latter point is likely related to changes in evaporation: while the spatial changes are targeting model biases, leading to a reduced MSE, the overall amplitude of the change is too large. **Changes in evaporation may be due to increased tropical convection.** The impact of this change in evaporation is seen most clearly in the energy budget, where both schemes significantly reduced the net surface energy from the relatively realistic levels attained in the deterministic model. However, it is critical to recall that these schemes have not been tuned, while the deterministic version of EC-Earth used as a reference has been extensively tuned, specifically when it comes to having a realistic energy budget. Tuning parameters for EC-Earth include constants that regulate processes such as entrainment and convection in the atmospheric case, and runoff in the LAND scheme case. In particular, the intensity and frequency of convection/runoff is modulated by these parameters, and tuned in a way to achieve realistic mean states. Non-linear impacts of stochastic schemes can lead to strong impacts on both the intensity and frequency of these processes, as our experiments have shown, and this significantly alters the mean state of the model.

It is therefore clear that the inclusion of a stochastic scheme must be treated in the same way as the inclusion of any other new parametrisation scheme, in that it will typically require a full re-calibration of the model parameters. By doing so, one may be able to obtain all the benefits to second-order diagnostics in the climate model in question (ENSO, the Asian monsoon, the MJO, European blocking, etc.) while still maintaining a realistic mean state and energy budget. In fact, given the improvements seen in key regional biases in our experiments, such a tuning procedure could potentially lead to a notably improved mean-state compared to a deterministic model. This will be examined further as part of the PRIMAVERA project, where these schemes will be tested in a fully coupled atmosphere-ocean framework. This work, presented in a future paper, will also include the stochastic ocean and sea-ice schemes and thereby examine the impact of adding stochasticity in every component.

*Code availability.* The EC-Earth source code is covered by a license through ECMWF, due to its use of the IFS as its atmospheric component. However, permission to use EC-Earth for research purposes can be obtained by requesting permission via the EC-Earth website <http://www.ec-earth.org>. The code itself is held on an SVN repository. The source code for all the stochastic schemes developed and used in this paper can be found in branch r4145-stochastic-ecearth in said repository. The branch of EC-Earth used to generate the simulations considered is titled r3345-oxtest1-isppt.

*Author contributions.* K.S. carried out and processed the EC-Earth simulations, analysed output, produced all figures except figure 9, wrote all sections except sections 2.2, 2.3 and 7.1, and prepared the manuscript for publication. H.M.C. developed and did initial testing of the ISPPT scheme, wrote section 2.2 and 7.1 and produced figure 9. D.M. developed and did initial testing of the stochastic land scheme, wrote section 2.3 and contributed to analysis of the impact on the hydrological budgets. S.J. contributed to analysis on the mean-state impact (sections 4.1, 5.1 and 6.1). T.N.P. secured the Horizon 2020 grant money instrumental for the undertaking of this project, and provided strategical oversight.

*Competing interests.* We declare there are no competing interests present.

*Acknowledgements.* K.S. and T.N.P. acknowledge funding from the European Commission under Grant Agreement 641727 of the Horizon  
5 2020 research programme. H.M.C. acknowledges funding from the Natural Environment Research Council under grant number NE/P018238/1. D.M. acknowledges funding from the EU-FP7 project SPECS (grant agreement 308378). S.J. is contributing to the project M3 of the Collaborative Research Centre TRR 181 "Energy Transfer in Atmosphere and Ocean" funded by the Deutsche Forschungsgemeinschaft (DFG, German Research Foundation) – Project number 274762653. We especially thank the Climate Prediction group at the Barcelona Supercomputing Center for providing initial condition files for our experiments.

## 10 References

- Arakawa, A. and Schubert, W. H.: Interaction of a cumulus cloud ensemble with the large scale environment, {P}art {I}, *J. Atmos. Sci.*, [https://doi.org/10.1175/1520-0469\(1974\)031<0674:IOACCE>2.0.CO;2](https://doi.org/10.1175/1520-0469(1974)031<0674:IOACCE>2.0.CO;2), 1974.
- Baldwin, M. P., Gray, L. J., Dunkerton, T. J., Hamilton, K., Haynes, P. H., Randel, W. J., Holton, J. R., Alexander, M. J., Hirota, I., Horinouchi, T., Jones, D. B., Kinnerson, J. S., Marquardt, C., Sato, K., and Takahashi, M.: The quasi-biennial oscillation, *Reviews of Geophysics*, 39, 179–229, <https://doi.org/10.1029/1999RG000073>, 2001.
- Balsamo, G., Beljaars, A., Scipal, K., Viterbo, P., van den Hurk, B., Hirschi, M., and Betts, A. K.: A Revised Hydrology for the ECMWF Model: Verification from Field Site to Terrestrial Water Storage and Impact in the Integrated Forecast System, *Journal of Hydrometeorology*, 10, 623–643, <https://doi.org/10.1175/2008JHM1068.1>, <http://journals.ametsoc.org/doi/abs/10.1175/2008JHM1068.1>, 2009.
- Bauer, P., Thorpe, A., and Brunet, G.: The quiet revolution of numerical weather prediction, <https://doi.org/10.1038/nature14956>, 2015.
- 20 Beljaars, A., e. a.: The numerics of physical parametrization, *Proc. of ECMWF Seminar on Recent Developments in Numerical Methods for Atmosphere and Ocean Modelling*, 2004.
- Bellprat, O., Massonnet, F., García-Serrano, J., Fučkar, N. S., Guemas, V., and Doblas-Reyes, F. J.: 8. The role of arctic sea ice and sea surface temperatures on the cold 2015 February over North America, *Bulletin of the American Meteorological Society*, 97, S36–S41, <https://doi.org/10.1175/BAMS-D-16-0159.1>, 2016.
- 25 Berner, J., Achatz, U., Batté, L., Bengtsson, L., De La Cámara, A., Weisheimer, A., Weniger, M., Williams, P. D., and Yano, J.-I.: Stochastic parameterizations: Toward a New View of Weather and Climate Models, *Bulletin of the American Meteorological Society*, 98, 565–588, <https://doi.org/10.1175/BAMS-D-15-00268.1>, <http://journals.ametsoc.org/doi/10.1175/BAMS-D-15-00268.1> { % } 0Ahttp://journals.ametsoc.org/doi/pdf/10.1175/BAMS-D-15-00268.1, 2017.
- Berner, J., Sardeshmukh, P. D., and Christensen, H. M.: On the dynamical mechanisms governing El Niño–Southern Oscillation irregularity, *Journal of Climate*, 31, 8401–8419, <https://doi.org/10.1175/JCLI-D-18-0243.1>, 2018.
- 30 Christensen, H. M.: Constraining stochastic parametrisation schemes using high-resolution simulations, for submission to *Q. J. R. Met. S.*, 2018.
- Christensen, H. M., Berner, J., Coleman, D. R., and Palmer, T. N.: Stochastic parameterization and El Niño-southern oscillation, *Journal of Climate*, 30, 17–38, <https://doi.org/10.1175/JCLI-D-16-0122.1>, 2017a.
- 35 Christensen, H. M., Lock, S. J., Moroz, I. M., and Palmer, T. N.: Introducing independent patterns into the Stochastically Perturbed Parametrization Tendencies (SPPT) scheme, *Quarterly Journal of the Royal Meteorological Society*, 143, 2168–2181, <https://doi.org/10.1002/qj.3075>, 2017b.
- Cloke, H. L., Pappenberger, F., and Renaud, J.-P.: Multi-method global sensitivity analysis (MMGSA) for modelling floodplainhydrological processes, *Hydrological Processes*, 22, 1660–1674, <https://doi.org/10.1002/hyp.6734>, <http://doi.wiley.com/10.1002/hyp.6734>, 2008.
- Cosby, B. J., Hornberger, G. M., Clapp, R. B., and Ginn, T. R.: A Statistical Exploration of the Relationships of Soil Moisture Characteristics to the Physical Properties of Soils, *Water Resources Research*, <https://doi.org/10.1029/WR020i006p00682>, 1984.
- 5 Davini, P., Von Hardenberg, J., Corti, S., Christensen, H. M., Juricke, S., Subramanian, A., Watson, P. A., Weisheimer, A., and Palmer, T. N.: Climate SPHINX: Evaluating the impact of resolution and stochastic physics parameterisations in the EC-Earth global climate model, *Geoscientific Model Development*, 10, 1383–1402, <https://doi.org/10.5194/gmd-10-1383-2017>, 2017.
- Dawson, A. and Palmer, T. N.: Simulating weather regimes: impact of model resolution and stochastic parameterization, *Climate Dynamics*, 44, 2177–2193, <https://doi.org/10.1007/s00382-014-2238-x>, 2015.

- 10 Dee, D. P., Uppala, S. M., Simmons, A. J., Berrisford, P., Poli, P., Kobayashi, S., Andrae, U., Balmaseda, M. A., Balsamo, G., Bauer, P., Bechtold, P., Beljaars, A. C., van de Berg, L., Bidlot, J., Bormann, N., Delsol, C., Dragani, R., Fuentes, M., Geer, A. J., Haimberger, L., Healy, S. B., Hersbach, H., Hólm, E. V., Isaksen, I., Kållberg, P., Köhler, M., Matricardi, M., McNally, A. P., Monge-Sanz, B. M., Morcrette, J. J., Park, B. K., Peubey, C., de Rosnay, P., Tavolato, C., Thépaut, J. N., and Vitart, F.: The ERA-Interim reanalysis: Configuration and performance of the data assimilation system, *Quarterly Journal of the Royal Meteorological Society*, 137, 553–597, <https://doi.org/10.1002/qj.828>, 2011.
- 15 Haarsma, R. J., Roberts, M. J., Vidale, P. L., Catherine, A., Bellucci, A., Bao, Q., Chang, P., Corti, S., Fučkar, N. S., Guemas, V., Von Hardenberg, J., Hazeleger, W., Kodama, C., Koenigk, T., Leung, L. R., Lu, J., Luo, J. J., Mao, J., Mizielinski, M. S., Mizuta, R., Nobre, P., Satoh, M., Scoccimarro, E., Semmler, T., Small, J., and Von Storch, J. S.: High Resolution Model Intercomparison Project (HighResMIP v1.0) for CMIP6, Geoscientific Model Development, <https://doi.org/10.5194/gmd-9-4185-2016>, 2016.
- 20 Hazeleger, W., Wang, X., Severijns, C., Ștefănescu, S., Bintanja, R., Sterl, A., Wyser, K., Semmler, T., Yang, S., van den Hurk, B., van Noije, T., van der Linden, E., and van der Wiel, K.: EC-Earth V2.2: Description and validation of a new seamless earth system prediction model, *Climate Dynamics*, 39, 2611–2629, <https://doi.org/10.1007/s00382-011-1228-5>, 2012.
- Hu, Y. and Fu, Q.: Observed poleward expansion of the Hadley circulation since 1979, *Atmospheric Chemistry and Physics*, 7, 5229–5236, <https://doi.org/10.5194/acp-7-5229-2007>, 2007.
- 25 Johanson, C. M. and Fu, Q.: Hadley cell widening: Model simulations versus observations, *Journal of Climate*, 22, 2713–2725, <https://doi.org/10.1175/2008JCLI2620.1>, 2009.
- Juricke, S. and Jung, T.: Influence of stochastic sea ice parametrization on climate and the role of atmosphere-sea ice-ocean interaction, *Philosophical Transactions of the Royal Society A: Mathematical, Physical and Engineering Sciences*, 372, <https://doi.org/10.1098/rsta.2013.0283>, 2014.
- 30 Juricke, S., Lemke, P., Timmermann, R., and Rackow, T.: Effects of stochastic ice strength perturbation on arctic finite element sea ice modeling, *Journal of Climate*, 26, 3785–3802, <https://doi.org/10.1175/JCLI-D-12-00388.1>, 2013.
- Juricke, S., Palmer, T. N., and Zanna, L.: Stochastic sub-grid scale ocean mixing: Impacts on low frequency variability, *Journal of Climate*, pp. JCLI-D-16-0539.1, <https://doi.org/10.1175/JCLI-D-16-0539.1>, 2017.
- Juricke, S., MacLeod, D., Weisheimer, A., and Palmer, T.: Seasonal to annual ocean forecasting skill and the role of model and observational uncertainty, *Quarterly Journal of the Royal Meteorological Society*, <https://doi.org/https://doi.org/10.1002/qj.3394>, 2018.
- 35 Leutbecher, M., Lock, S. J., Ollinaho, P., Lang, S. T., Balsamo, G., Bechtold, P., Bonavita, M., Christensen, H. M., Diamantakis, M., Dutra, E., English, S., Fisher, M., Forbes, R. M., Goddard, J., Haiden, T., Hogan, R. J., Juricke, S., Lawrence, H., MacLeod, D., Magnusson, L., Malardel, S., Massart, S., Sandu, I., Smolarkiewicz, P. K., Subramanian, A., Vitart, F., Wedi, N., and Weisheimer, A.: Stochastic representations of model uncertainties at ECMWF: state of the art and future vision, <https://doi.org/10.1002/qj.3094>, 2017.
- Lord, S. J., Chao, W. C., and Arakawa, A.: Interaction of a Cumulus Cloud Ensemble with the Large-Scale Environment. Part IV: The Discrete Model, *Journal of the Atmospheric Sciences*, 39, 104–113, [https://doi.org/10.1175/1520-0469\(1982\)039<0104:IOACCE>2.0.CO;2](https://doi.org/10.1175/1520-0469(1982)039<0104:IOACCE>2.0.CO;2), [http://journals.ametsoc.org/doi/abs/10.1175/1520-0469\(1982\)039<0104:IOACCE>2.0.CO;2](http://journals.ametsoc.org/doi/abs/10.1175/1520-0469(1982)039<0104:IOACCE>2.0.CO;2), 1982.
- 5 MacLeod, D., Cloke, H., Pappenberger, F., and Weisheimer, A.: Evaluating uncertainty in estimates of soil moisture memory with a reverse ensemble approach, *Hydrology and Earth System Sciences*, 20, 2737–2743, <https://doi.org/10.5194/hess-20-2737-2016>, 2016.
- Macleod, D. A., Cloke, H. L., Pappenberger, F., and Weisheimer, A.: Improved seasonal prediction of the hot summer of 2003 over Europe through better representation of uncertainty in the land surface, *Quarterly Journal of the Royal Meteorological Society*, 142, 79–90, <https://doi.org/10.1002/qj.2631>, 2016.

- 10 Mitas, C. M. and Clement, A.: Has the Hadley cell been strengthening in recent decades?, *Geophysical Research Letters*, 32, 1–5, <https://doi.org/10.1029/2004GL021765>, 2005.
- Numaguti, A.: Dynamics and Energy Balance of the Hadley Circulation and the Tropical Precipitation Zones: Significance of the Distribution of Evaporation, *Journal of the Atmospheric Sciences*, [https://doi.org/10.1175/1520-0469\(1993\)050<1874:DAEBOT>2.0.CO;2](https://doi.org/10.1175/1520-0469(1993)050<1874:DAEBOT>2.0.CO;2), 1993.
- Orth, R., Dutra, E., and Pappenberger, F.: Improving Weather Predictability by Including Land Surface Model Parameter Uncertainty, *Monthly Weather Review*, 144, 1551–1569, <https://doi.org/10.1175/MWR-D-15-0283.1>, <http://journals.ametsoc.org/doi/10.1175/MWR-D-15-0283.1>, 2016.
- 15 Palmer, T., Buizza, R., Jung, T., Leutbecher, M., Shutts, G. J., Steinheimer, M., and Weisheimer, A.: Stochastic Parameterization and Model Uncertainty, vol. 598, <http://www.ecmwf.int/publications/>, 2009.
- Palmer, T. N.: Towards the probabilistic Earth-system simulator: A vision for the future of climate and weather prediction, *Quarterly Journal of the Royal Meteorological Society*, 138, 841–861, <https://doi.org/10.1002/qj.1923>, 2012.
- 20 Palmer, T. N., Shutts, G. J., Hagedorn, R., Doblas-Reyes, F., Jung, T., and M. Leutbecher: Representing model uncertainty in weather and climate prediction, *Ann. Rev. Earth Planet. Sci.*, 33, 163–193, 2005.
- Rackow, T. and Juricke, S.: A flow-dependent stochastic coupling scheme for climate models with high ocean-to-atmosphere resolution ratio, Submitted to *Journal of Advances in Modeling Earth Systems*, 2019.
- 25 Seager, R., Ting, M., Held, I., Kushnir, Y., Lu, J., Vecchi, G., Huang, H. P., Harnik, N., Leetmaa, A., Lau, N. C., Li, C., Velez, J., and Naik, N.: Model projections of an imminent transition to a more arid climate in southwestern North America, *Science*, 316, 1181–1184, <https://doi.org/10.1126/science.1139601>, 2007.
- Seidel, D. J. and Randel, W. J.: Recent widening of the tropical belt: Evidence from tropopause observations, *Journal of Geophysical Research Atmospheres*, 112, <https://doi.org/10.1029/2007JD008861>, 2007.
- 30 Shao, Y. and Irannejad, P.: On the choice of soil hydraulic models in land-surface schemes, *Boundary-Layer Meteorology*, 90, 83–115, <https://doi.org/10.1023/A:1001786023282>, 1999.
- Strømmer, K., Christensen, H. M., Berner, J., and Palmer, T. N.: The impact of stochastic parametrisations on the representation of the Asian summer monsoon, *Climate Dynamics*, 0, 1–14, <https://doi.org/10.1007/s00382-017-3749-z>, 2017.
- Trenberth, K. E., Fasullo, J. T., and Kiehl, J.: Earth’s global energy budget, *Bulletin of the American Meteorological Society*, 90, 311–323, <https://doi.org/10.1175/2008BAMS2634.1>, 2009.
- 35 Uppala, S. M., Kallberg, P. W., Simmons, A. J., Andrae, U., Bechtold, V. D. C., Fiorino, M., Gibson, J. K., Haseler, J., Hernandez, A., Kelly, G. A., Li, X., Onogi, K., Saarinen, S., Sokka, N., Allan, R. P., Andersson, E., Arpe, K., Balmaseda, M. A., Beljaars, A. C. M., Berg, L. V. D., Bidlot, J., Bormann, N., Caires, S., Chevallier, F., Dethof, A., Dragosavac, M., Fisher, M., Fuentes, M., Hagemann, S., Hólm, E., Hoskins, B. J., Isaksen, L., Janssen, P. A. E. M., Jenne, R., McNally, A. P., Mahfouf, J.-F., Morcrette, J.-J., Rayner, N. A., Saunders, R. W., Simon, P., Sterl, A., Trenberth, K. E., Untch, A., Vasiljevic, D., Viterbo, P., and Woollen, J.: The ERA-40 re-analysis, *Quarterly Journal of the Royal Meteorological Society*, 131, 2961–3012, <https://doi.org/10.1256/qj.04.176>, <http://doi.wiley.com/10.1256/qj.04.176>, 2005.
- 5 van Genuchten, M. T.: A Closed-form Equation for Predicting the Hydraulic Conductivity of Unsaturated Soils<sup>1</sup>, *Soil Science Society of America Journal*, 44, 892, <https://doi.org/10.2136/sssaj1980.03615995004400050002x>, <https://www.soils.org/publications/sssaj/abstracts/44/5/SS0440050892>, 1980.
- Waliser, D. E., Shi, Z., Lanzante, J. R., and Oort, A. H.: The Hadley circulation: Assessing NCEP/NCAR reanalysis and sparse in-situ estimates, *Climate Dynamics*, 15, 719–735, <https://doi.org/10.1007/s003820050312>, 1999.

- 10 Wang, Y. and Zhang, G. J.: Global climate impacts of stochastic deep convection parameterization in the NCAR CAM5, *Journal of Advances in Modeling Earth Systems*, 8, 1641–1656, <https://doi.org/10.1002/2016MS000756>, 2016.
- Watson, P. A. G., Berner, J., Corti, S., Davini, P., von Hardenberg, J., Sanchez, C., Weisheimer, A., and Palmer, T. N.: The impact of stochastic physics on tropical rainfall variability in global climate models on daily to weekly timescales, *Journal of Geophysical Research: Atmospheres*, 122, 5738–5762, <https://doi.org/10.1002/2016JD026386>, <http://doi.wiley.com/10.1002/2016JD026386>, 2017.
- 665 Weisheimer, A., Palmer, T. N., and Doblas-Reyes, F. J.: Assessment of representations of model uncertainty in monthly and seasonal forecast ensembles, *Geophysical Research Letters*, 38, <https://doi.org/10.1029/2011GL048123>, 2011.
- Williams, P. D.: Climatic impacts of stochastic fluctuations in air-sea fluxes, *Geophysical Research Letters*, <https://doi.org/10.1029/2012GL051813>, 2012.
- Yang, C., Christensen, H., Corti, S., von Hardenberg, J., and Davini, P.: The impact of stochastic physics on the El Niño Southern Oscillation  
670 in the EC-Earth coupled model, Submitted to *Climate Dynamics*, 2018.

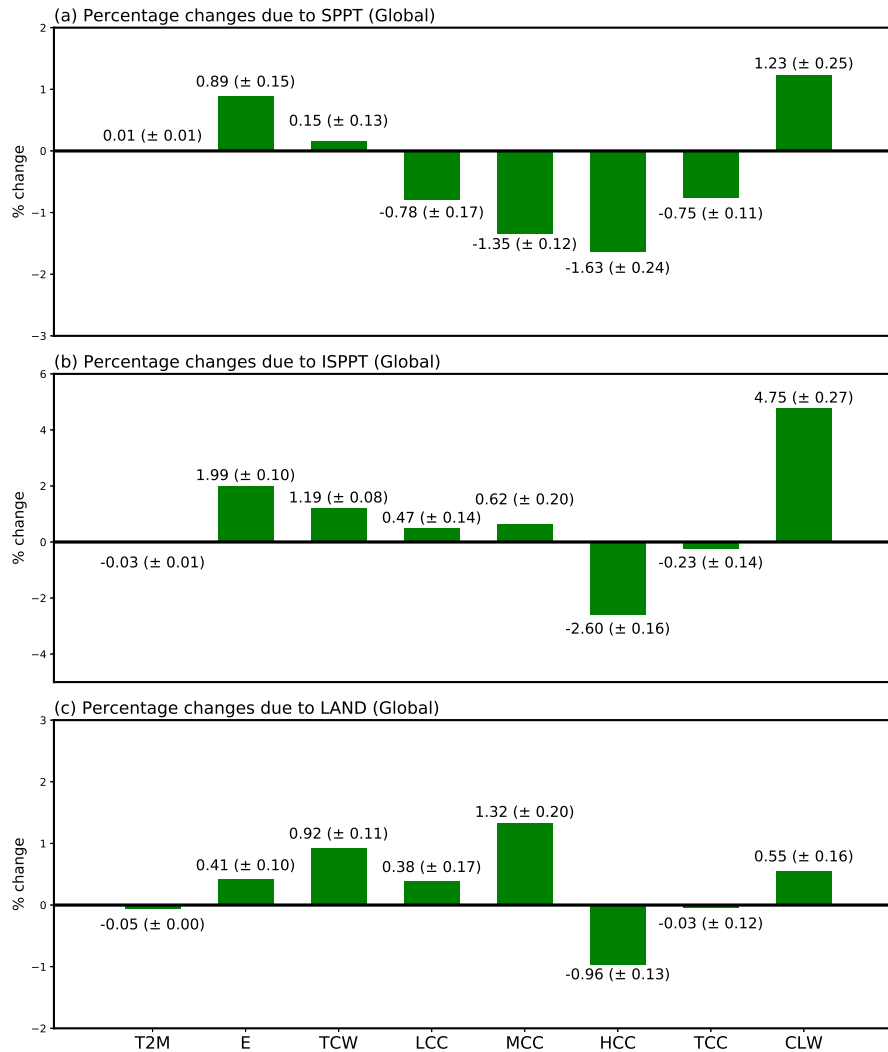


**Figure 1.** Average percentage change, relative to CTRL, in global mean of (a) SPPT simulations, (b) ISPPT and (c) LAND. Variables shown are, in order, two-meter temperature (T2M), evaporation (E), total column water (TCW), low cloud cover (LCC), mid-level cloud cover (MCC), high-level cloud cover (HCC), total cloud cover (TCC) and cloud liquid water (CLW). Uncertainty estimates are twice the standard deviation of the five individual differences. Note: due to conservation of water, the change in precipitation (not shown) is almost exactly equal to the change in evaporation.

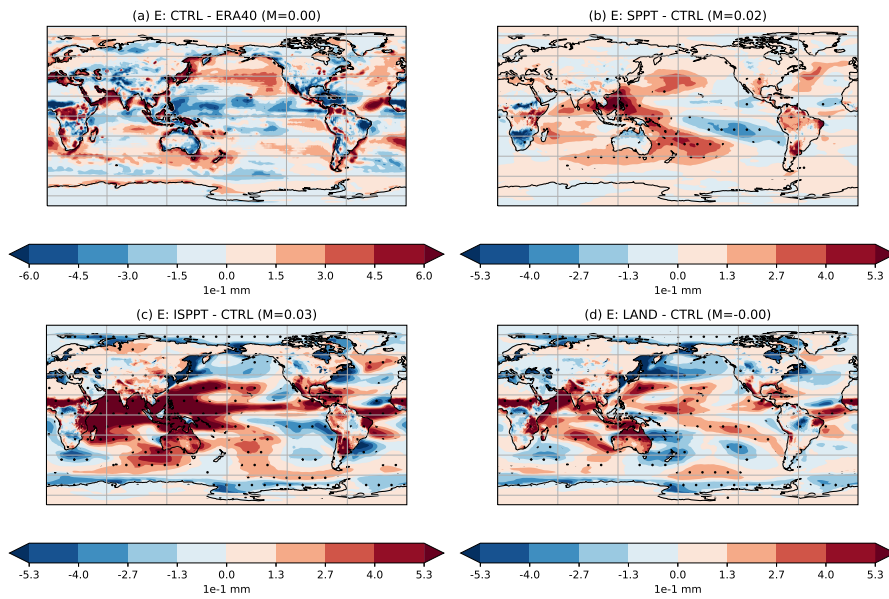


**Figure 2.** Mean differences in evaporation between (a) CTRL and ERA40, (b) SPPT and CTRL, (c) ISPT and CTRL and (d) LAND and CTRL. Stippling indicates regions where the difference is statistically significant to the 95% confidence interval, as measured by a two-tailed T-test. In each panel, M denotes the mean of the difference. Note the difference in scales between (a) and (b)-(c)-(d).

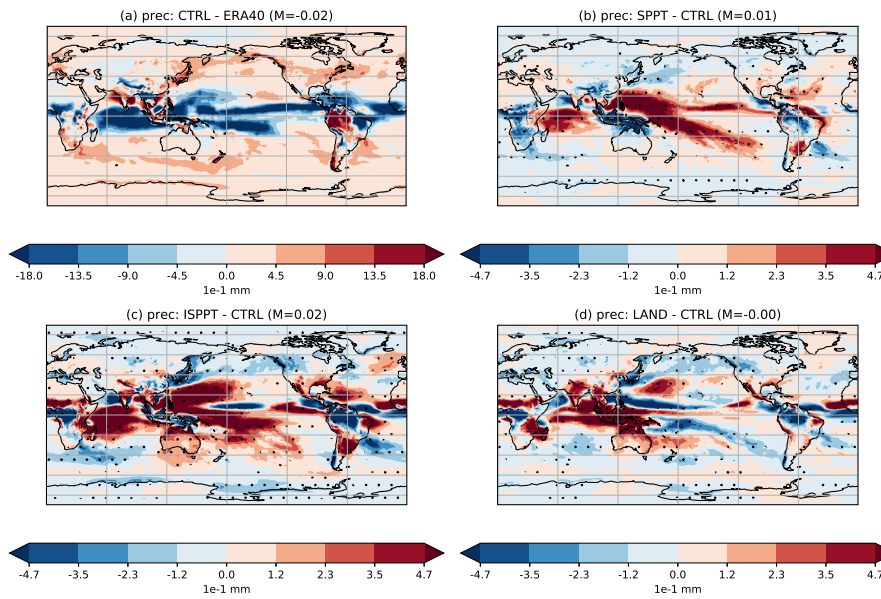


**Figure 3.** Mean differences in precipitation between (a) CTRL and ERA40, (b) SPPT and CTRL, (c) ISPPT and CTRL and (d) LAND and CTRL. Stippling indicates regions where the difference is statistically significant to the 95% confidence interval, as measured by a two-tailed T-test. In each panel, M denotes the mean of the difference. Note the difference in scales between (a) and (b)-(c)-(d).

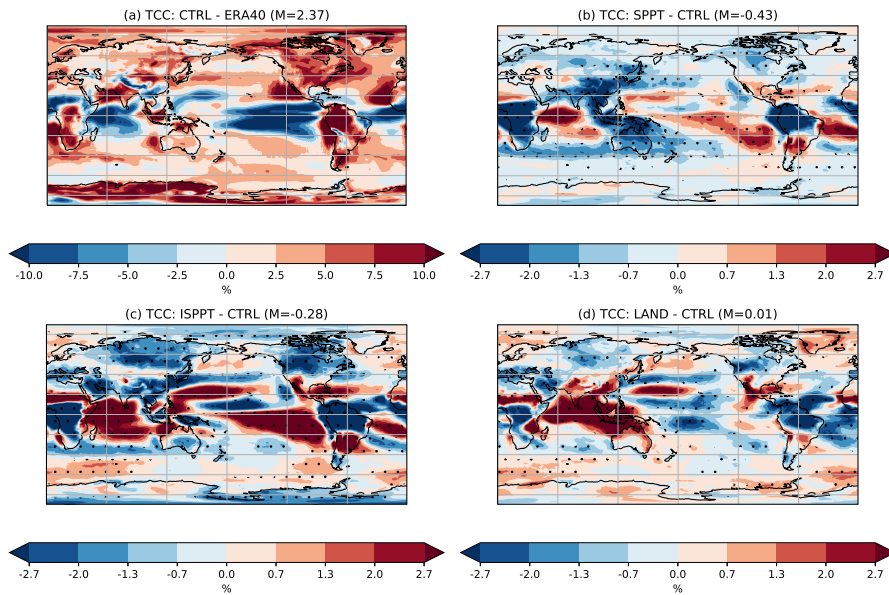


**Figure 4.** Mean differences in total cloud cover between (a) CTRL and ERA40, (b) SPPT and CTRL, (c) ISPPT and CTRL and (d) LAND and CTRL. Stipling indicates regions where the difference is statistically significant to the 95% confidence interval, as measured by a two-tailed T-test. In each panel, M denotes the mean of the difference. Note the difference in scales between (a) and (b)-(c)-(d). The units of % indicate the proportion of the column occupied by clouds.

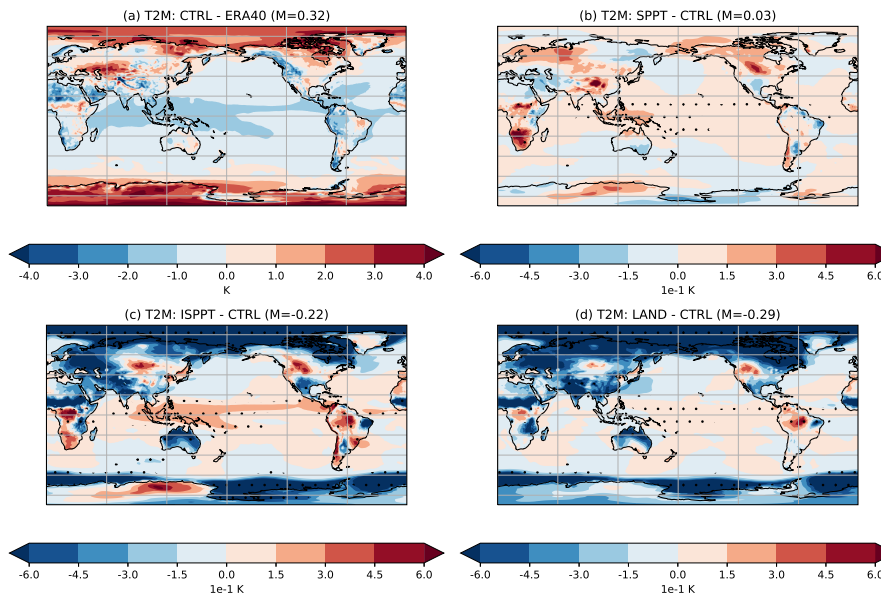


**Figure 5.** Mean differences in two-meter temperature between (a) CTRL and ERA40, (b) SPPT and CTRL, (c) ISPPT and CTRL and (d) LAND and CTRL. Stippling indicates regions where the difference is statistically significant to the 95% confidence interval, as measured by a two-tailed T-test. In each panel, M denotes the mean of the difference. Note the difference in scales between (a) and (b)-(c)-(d).

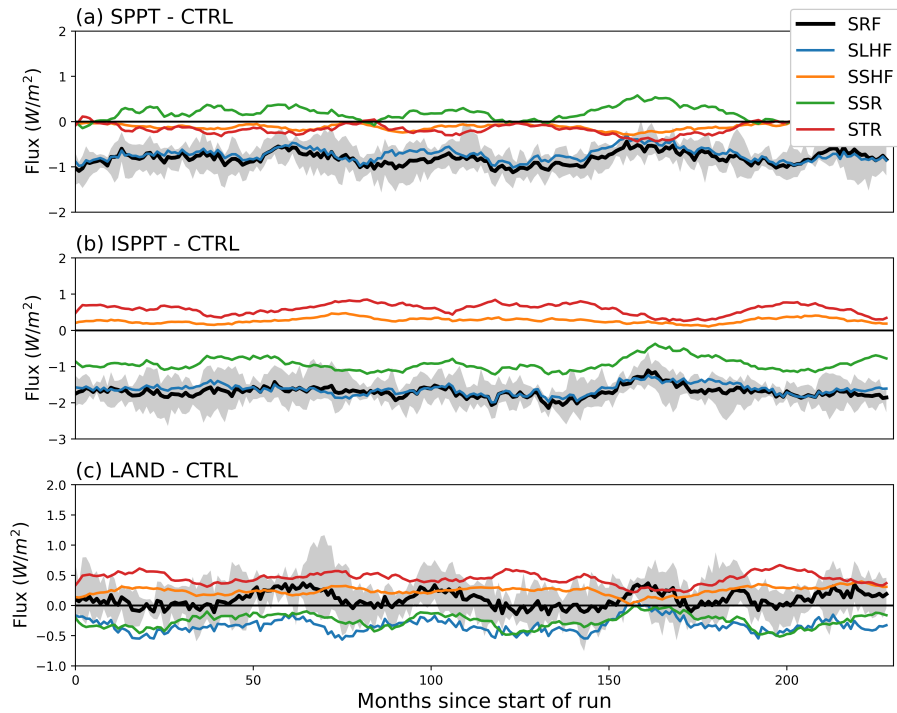


**Figure 6.** Global mean time series of energy fluxes for (a) SPPT minus CTRL, (b) ISPPT minus CTRL, and (c) LAND minus CTRL. Fluxes shown are latent heat flux (SLHF, blue), sensible heat flux (SSHF, orange), surface thermal radiation (STR, red), surface solar radiation (SSR, green) and net surface energy (SRF, black). Note the IFS convention that downward fluxes are positive and upward fluxes (such as sensible and latent heat flux) are negative. SRF is the sum of the other fluxes. The black shading captures two standard deviations around the SRF mean as sampled from the five individual differences. Timeseries have been smoothed with a 12-month running mean to remove the seasonal cycle.

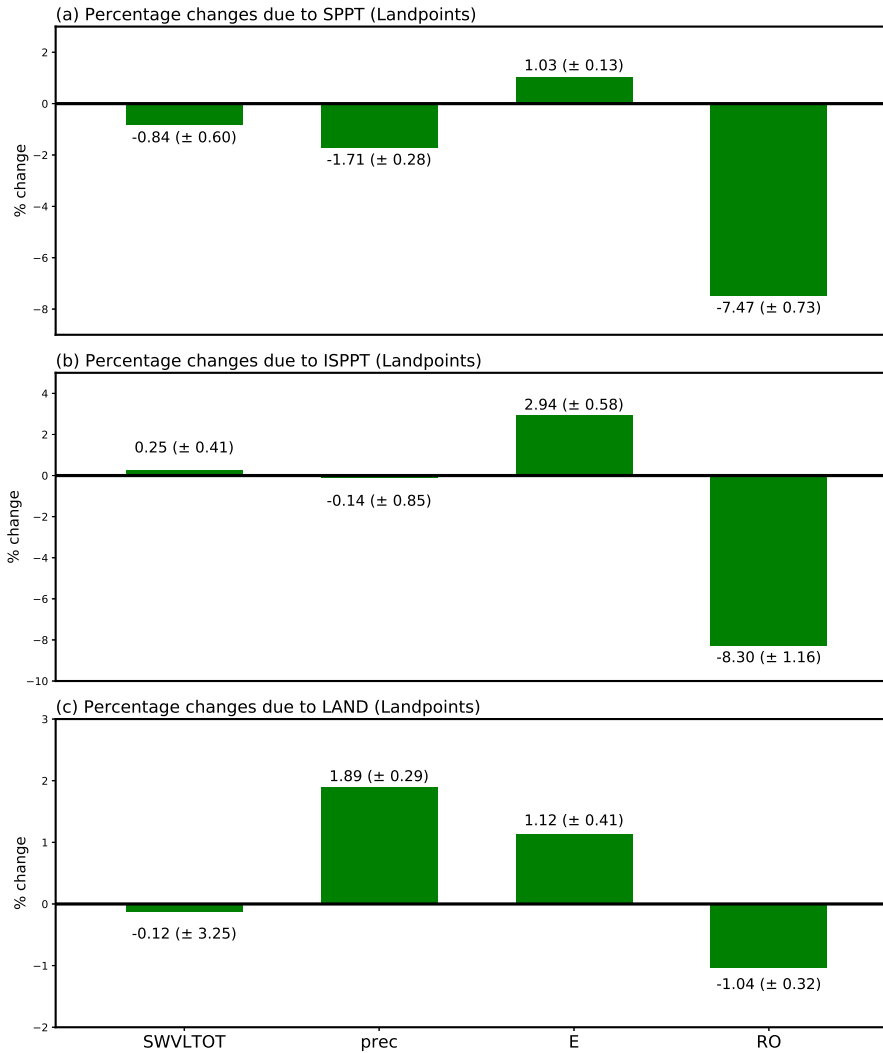


**Figure 7.** Average percentage change, relative to CTRL, in global mean of (a) SPPT simulations, (b) ISPPT and (c) LAND. All data was restricted to land-points only. For LAND, Antarctica was also excluded. Variables shown are, in order, total soil water content (SWVLTOT), precipitation (prec), evaporation (E) and runoff (RO). Uncertainty estimates are twice the standard deviation of the five individual differences.

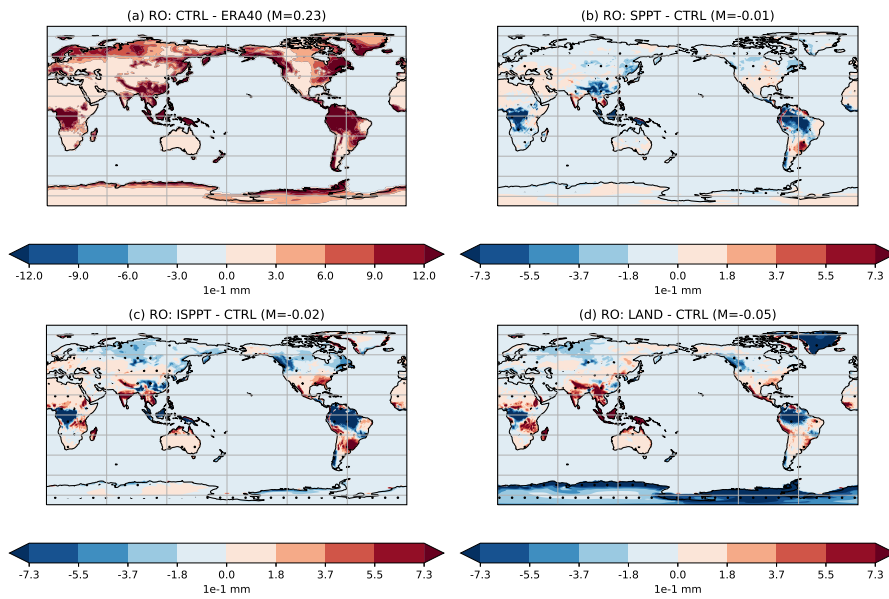


**Figure 8.** Mean differences in runoff between (a) CTRL and ERA40, (b) SPPT and CTRL, (c) ISPT and CTRL and (d) LAND and CTRL. Stipling indicates regions where the difference is statistically significant to the 95% confidence interval, as measured by a two-tailed T-test. In each panel, M denotes the mean of the difference. Note the difference in scales between (a) and (b)-(c)-(d).

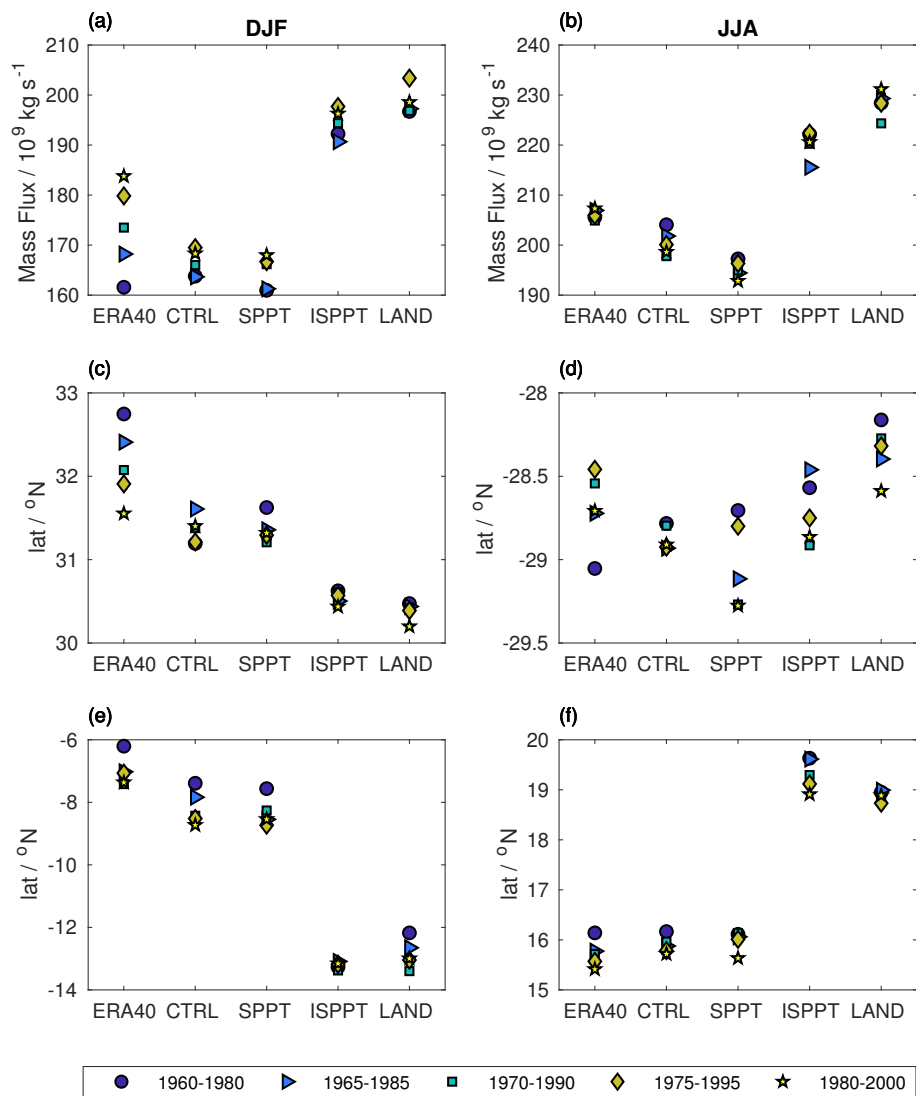


**Figure 9.** Impact of stochastic parametrizations on the Hadley circulation. The magnitude of the overturning circulation indicated by the maximum of the streamfunction of the dominant cell in (a) DJF and (b) JJA for each scheme. The latitude of the downwelling branch of the dominant (winter hemisphere) cell in (c) DJF and (d) JJA. The latitude of the upwelling branch of the dominant (winter hemisphere) cell in (e) DJF and (f) JJA. The data diagnostic is shown for each of the five AMIP simulations in turn, the darker colours indicate earlier years, ranging from dark blue (1960–1980) to yellow (1980–2000).

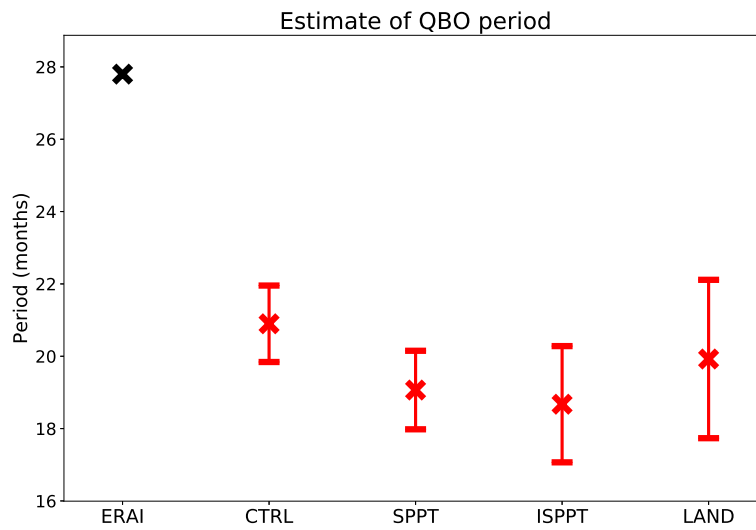


**Figure 10.** Estimates of the QBO period, as measured using equatorial zonal winds at 50hPa. The red crosses show, for each scheme, the mean across the five estimates (computed from the five ensemble members), and the errorbars capture twice the standard error of this mean estimate. The reanalysis product ERA-Interim is shown in black for comparison.

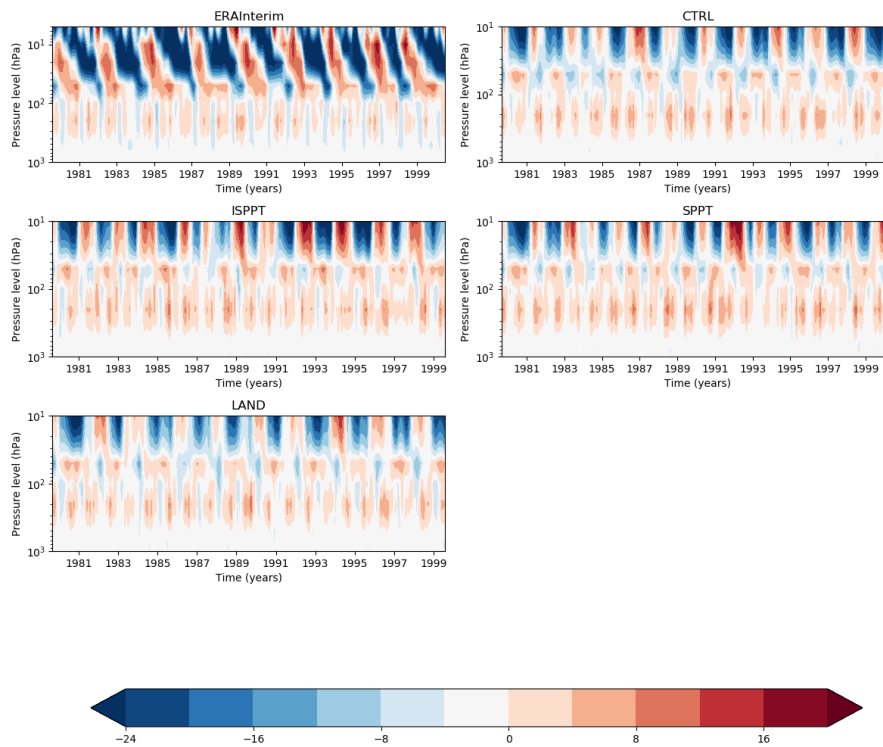


**Figure 11.** Visualisation of the QBO (time-pressure level section of zonal winds between 10S and 10N with the seasonal mean removed) for the ensemble member covering 1980-2000, the period overlapping the most with ERA-Interim. Pressure levels are plotted according to a logarithmic scale for ease of interpretation. Units are  $m s^{-1}$ .

**Table 1.** Globally averaged surface energy fluxes for the CTRL simulation. The values in the Observed row are the estimates from (Trenberth et al., 2009) for the period 2000-2004. STR = net surface thermal radiation, SSR = net surface solar radiation, SLHF = surface latent heat flux, SSHF = surface sensible heat flux, SRF = net surface energy. Units are  $W/m^2$  in all cases.

	STR	SSR	SLHF	SSHF	SRF
1991-1995	61.2	163.8	82.7	19.3	0.6
1991-2000	61.1	164.2	82.8	19.4	1.0
Observed	63	161	80	17	0.9

**Table 2.** Mean-square errors between the spatial means of reanalysis (ERA40) and each EC-Earth configuration (CTRL, SPPT, ISPPT and LAND) for T2M (two-meter temperature), T (temperature) at various levels (hPa), Prec (precipitation), E (evaporation), TCC (total cloud cover), RO (total runoff), TCW (total column water), SWS (10 meter wind speeds) and U (zonal winds) at different pressure levels (hPa). Values where a stochastic scheme significantly reduced the error (see section 3.2) have been bolded.

	CTRL	SPPT	ISPPT	LAND
T2M	2.545	2.551	<b>1.940</b>	<b>1.851</b>
T1000	1.745	1.779	<b>1.211</b>	<b>1.065</b>
T850	1.694	1.794	1.614	<b>1.202</b>
T200	3.989	<b>3.669</b>	<b>3.481</b>	<b>3.506</b>
T100	5.802	5.753	4.844	5.013
T10	27.543	27.329	43.580	28.512
Prec	0.809	<b>0.754</b>	<b>0.724</b>	<b>0.764</b>
E	0.071	0.075	<b>0.065</b>	<b>0.059</b>
TCC	0.0035	<b>0.0030</b>	<b>0.0028</b>	0.0035
RO	0.457	<b>0.393</b>	<b>0.366</b>	<b>0.405</b>
TCW	1.454	1.471	1.546	1.557
SWS	0.445	0.463	0.479	0.448
U1000	0.464	0.500	0.4636	<b>0.418</b>
U850	0.699	0.781	0.735	<b>0.605</b>
U200	2.667	4.026	3.834	<b>2.038</b>
U100	2.912	3.033	3.111	2.491
U10	10.073	14.394	14.641	9.834